

Multi-spectral and Thermography Imaging Techniques for the Investigation of a 15th Century Wall Painting

Marco Ricci

University of Calabria: Universita della Calabria

Stefano Laureti

University of Calabria: Universita della Calabria

Hamed Malekmohammadi

University of Perugia

Stefano Sfarra

University of L'Aquila

Marcello Melis

Profilocolore srl

Giorgia Agresti

University of Tuscia

Luca Lanteri

University of Tuscia

Claudia Colantonio

University of Tuscia

Giuseppe Calabrò

University of Tuscia

Claudia Pelosi (✉ pelosi@unitus.it)

Department of Economics, Engineering, Society and Business Organization (DEIM), University of Tuscia, 12 Viterbo, Italy; <https://orcid.org/0000-0002-1338-5267>

Research article

Keywords: Hypercolorimetric multispectral imaging, Pulse-Compression Thermography, wall 42 paintings, restoration, underdrawing, painting stratigraphy

Posted Date: October 29th, 2020

DOI: <https://doi.org/10.21203/rs.3.rs-97372/v1>

License: © ⓘ This work is licensed under a Creative Commons Attribution 4.0 International License.

[Read Full License](#)

Multi-spectral and thermography imaging techniques for the investigation of a 15th century wall painting

Marco Ricci¹, Stefano Laureti¹, Hamed Malekmohammadi², Stefano Sfarra³, Marcello Melis⁴,
Giorgia Agresti⁵, Luca Lanteri⁵, Claudia Colantonio⁵, Giuseppe Calabrò⁵, Claudia Pelosi^{5*}

¹ Department of Informatics, Modeling, Electronics and Systems Engineering, University of Calabria, Rende (CS), Italy; marco.ricci@unical.it; stefano.laureti@unical.it

² Department of Engineering, Polo Scientifico Didattico di Terni, University of Perugia, Terni, Italy; hamed.malekmohammadi@unipg.it

³ Department of Industrial and Information Engineering and Economics, University of L'Aquila, L'Aquila, Italy; stefano.sfarra@univaq.it

⁴ Profilocolore S.r.l., Rome, Italy; marcello.melis@profilocolore.it

⁵ Department of Economics, Engineering, Society and Business Organization (DEIM), University of Tuscia, Viterbo, Italy; agresti@unitus.it; llanteri@unitus.it; c.colantonio@unitus.it; giuseppe.calabro@unitus.it; pelosi@unitus.it

* Correspondence: pelosi@unitus.it; Tel.: +39-333-2877468 (C.P.)

Abstract: When planning the restoration of an artwork, the good practice involves the evaluation of the item healthiness before starting the common operation of cleaning, consolidation, etc., possibly through non-invasive techniques that supply meaningful information about the whole item. Motivated by this need, a plethora of imaging techniques are used in cultural heritage diagnostic typically borrowed from other applications – e.g. medical diagnostics, nondestructive testing, etc., and then tailored for inspecting cultural heritage objects. In the inspection of a painting, hyper- and multi- spectral techniques are commonly used to analyze the outer layers (varnish, pictorial and drawing) while X-ray, tomography, and many other can be employed to investigate its inner structure. Although highly desirable, a single technique providing all the info about a painting is still not available, thus it is of great interest defining protocols that could optimally exploit the complementarities of a limited number of techniques. To this aim, the present paper shows the combined use of the Hypercolorimetric Multispectral Imaging (HMI) and that of the Pulse-Compression Thermography (PuCT) on a 15th century wall painting attributed to the Italian artist Antonio del Massaro, also known as Pastura, and representing the Madonna with the Child and the Saints Jerome and Francis. In particular, HMI is a multispectral imaging method working from the ultraviolet to the near infrared region, exploiting advanced processing based on artificial intelligence to define hypercolorimetric coordinates. Such approach guarantees a thorough

34 analysis of the outer layers, underlining previous restorations, varnish alterations and allowing the
35 pigments to be classified from a comparison with a large database. The PuCT method adopted here
36 has been tailored for the specific needs of artworks' inspection and it allows for a safe imaging of
37 the multilayer structure of paintings, and hence the stratigraphy analysis, through a suitable
38 processing of the time-domain thermal response. The capabilities and the complementarities of the
39 two techniques, whose info can also be fused through postprocessing techniques, are illustrated in
40 detail in this paper. A false-color imaging approach is also proposed to improve the readability and
41 analysis of the thermography results.

42 **Keywords:** Hypercolorimetric multispectral imaging; Pulse-Compression Thermography; wall
43 paintings; restoration; underdrawing; painting stratigraphy.

44

45 1. Introduction

46 In developing restoration, conservation and preservation plans for Cultural Heritage (CH)
47 items, diagnostics is nowadays a key ingredient. The knowledge of both the original and restoration
48 materials, of the construction techniques, and of the stratigraphy of the artwork is requested by
49 conservators to define any potential interventions. Among numerous diagnostics tools, imaging
50 techniques have become widely applied in CH as they provide information on the materials and the
51 structure of the artworks in a non-invasive and non-destructive way. Such information is useful for
52 conservators to choose the most appropriate intervention decision during a restoration work [1-16].
53 Imaging techniques can provide a complete knowledge of the surfaces in a fast and reliable way
54 without the need for sampling micro-chips of materials for laboratory analysis, a fact that is in
55 general highly desirable or mandatory in some cases [13-16].

56 When dealing with paintings, a thorough diagnostic approach relies on (i) the integration of
57 data collected from different imaging techniques, (ii) the exploitation of their complementarities in
58 terms of spectral range and/or physical principles, and (iii) the potential combination of the relative

59 outputs via digital imaging processing tools. It is important to note that data integration and fusion
60 can strongly support traditional analytical methods, yielding a comprehensive diagnosis of the
61 painting state of conservation and reducing any ambiguities due to the use of a single diagnostic
62 method [2,9-11,14,16-17].

63 Hyperspectral (HS), multispectral (MS), and any other imaging techniques processing spectral
64 data are the preferred ones for studying the outer layers of painting such as the varnish, the pictorial
65 stratum, the dirt — if present — and the underdrawings. Thus, starting from ultraviolet (UV),
66 passing by visible (VIS), and reaching infrared (IR), the outer layers of a painting can be inspected. In
67 particular, UV reflectance and fluorescence are employed for evaluating the condition of the varnish
68 layer, for identifying possible retouching and over-paintings; fluorescence can also aid in the
69 characterization of the materials (varnish, pigments and binders). The analysis of the reflected light
70 in the VIS range, especially using raking light, highlights the artist's technique (brushstrokes,
71 impastos), the presence of flaking paint or cracks, and it can also show areas requiring special care
72 for being faithfully preserved. Finally, images in the near IR range are used for the analysis of the
73 inner layers — near IR light can penetrate the pictorial layer and make the underdrawing and
74 possible *pentimenti* being visible due to the high reflectance of carbon-based materials. This is
75 possible since most of the historical pigments, binders, and varnish are partially transparent in the
76 near IR (around 1000 nm of wavelength). However, the transparency of the outer layers to the near
77 IR lights depends on many factors such as the layer thickness and chemical composition, a fact that
78 makes the imaging of the underdrawing layer challenging. Another powerful exploitation of the IR
79 radiation for painting analysis is represented by the HS imaging techniques that use the retrieved
80 pixelwise spectral information to classify the pigments and to map them over the inspected painting
81 surface. Hyperspectral cameras split the range of sensitivity of the sensors in hundreds of bins for an
82 accurate reconstruction of the reflected IR spectrum. In painting inspections, near (900-1700 nm) or
83 short-wave (1000-2500 nm) IR hyperspectral camera are mainly used — many of the overtones and
84 the combination of vibrational bands characteristics of the inorganic pigments used in historical

85 paintings fall in these ranges. It should be noted that the application of HS imaging in the middle
86 (3000-5000 nm) IR has also been recently reported to classify organic compounds [18].

87 The main drawback of HS imaging is a practical one: hyperspectral cameras are still very
88 expensive and need for a scanning stage to output images of the surface — the spectral scanning is
89 usually realized by combining a standard IR camera with a monochromator or with a diffraction
90 grating. These facts hamper the use of HS imaging for in situ artworks inspection. Further, for what
91 mentioned above, HS imaging should be anyway combined with UV and VIS imaging methods. As
92 a consequence, the possible engineering of a single technique capable of providing info within the
93 mentioned electromagnetic spectra is highly desirable and would be of a great value from a practical
94 point of view. In this framework, HMI processes information from the near UV to the near IR. The
95 here-employed system relies on a 36 megapixels reflex Nikon camera modified to work in the
96 300-1000 nm extended range combined with proper choice of flash lamps and optical filters. The
97 images obtained are then represented into a 7D hyper-colorimetric space. Such coordinate system
98 extends the concept of the common 3D colour space used in colorimetry, i.e. the CIE XYZ standard,
99 or the more common RGB, by defining seven hyper-colorimetric coordinates in which a coordinate
100 is related to the near UV range and three ones to the near IR range. By combining artificial
101 intelligence techniques with a proper calibration procedure, it is possible to fully exploit this
102 augmented colour space to perform all the tasks discussed above [19-21].

103 Regarding the evaluation of the whole painting stratigraphy, i.e. from the varnish to the
104 support (panel, canvas, wall, etc.), the number of possible techniques is even larger: X-ray imaging
105 is largely employed, 2D and 3D XRF imaging are often used for identifying materials' chemical
106 composition. In addition, medical computer tomography techniques, terahertz time resolved (TTR)
107 imaging, optical coherence tomography (OCT) and nuclear magnetic resonance have recently
108 enlarged the range of methods for such purpose [22-24].

109 In this framework, InfraRed Thermography (IRT) represents a robust technique for the
110 inspection of CH items [25-26]. Also in this case, a trade-off between information amount, cost and

111 measurement complexity (measurement time, mechanical equipment, computational costs, etc.)
112 should be found. IRT is relatively easy to be performed in situ, providing imaging without the need
113 of imaging reconstruction algorithms and it can be operated on large areas moderately easy.
114 Moreover, IRT does not require a continuous translation stage as for the point-wise imaging
115 equipment such as TTR, XRF, OCT, NMR, etc., and it does not involve any hazardous source. The
116 costs are not as low as the typical equipment for IR reflectometry, but are among the cheapest ones
117 within the above-mentioned techniques.

118 On the other hand, IRT does not reach the depth resolution of other techniques such as TTR and
119 OCT, but it can inspect the support up to depth of several millimetres — a few centimetres in the
120 case of wall paintings provided that a suitable excitation scheme is used. In addition, recent
121 developments in IRT technique have increased its effectiveness for artworks inspection and reduced
122 the risk of any alteration of the artworks due to the thermal stimulus [27-28]. In particular, the use of
123 the so-called Pulse-Compression Thermography (PuCT) procedure combined with a pseudo-noise
124 modulated heating stimuli demonstrated to be effective even with a very small increment in the
125 sample surface's temperature ($\sim 1^\circ\text{C}$) [29-30].

126 For the mentioned reasons, the combined use of PuCT and HMI is very promising for in situ
127 inspections of paintings: the tailored hardware and the advanced processing and postprocessing
128 algorithms provide complimentary information to art historians and restorers, and their contextual
129 use allows for investigating the paintings' stratigraphy from the varnish to the support. The output
130 of the two methods can be easily fused by image processing tools and post-processing algorithms.

131 The first example of the combined application of the two techniques was recently reported in
132 the literature — HMI and PuCT were used for inspecting two historical panel paintings of the
133 renaissance period, realised by Andrea Mantegna and from Michelangelo's workshop [31].

134 In the present work, HMI and PuCT are applied together for the first time on a detached wall
135 painting under restoration in the Laboratories of the five-year course in Conservation and
136 Restoration of Cultural Heritage (LMR/02) of University of Tuscia, Italy [32].

137 The wall painting, specifically a lunette, depicts a Madonna and Child enthroned in between
138 the angels, and the Saints Jerome and Francis (Fig. 1). The painting has been dated back to 1490 and
139 it is attributed to the artist Antonio del Massaro, known as Pastura (1450-1519). Originally, it was in
140 the convent of *Santa Maria del Paradiso* in Viterbo, central Italy [33-34].

141 After the detachment occurred in 1912, the painting was transferred in the Civic Museum of
142 Viterbo during the opening day of the new seat in Santa Maria della Verità church. The detachment
143 of the lunette was probably due to its bad state of conservation caused by the exposure to
144 weathering and acts of vandalism [35]. In fact, large grouts are visible in the photographs of the
145 beginning of 20th century confirming its bad state of conservation and the need for interventions [36].

146 The ancient restoration interventions were made with both unsuitable materials and techniques
147 such as the mimetic reintegration, hampering in turn the correct readability of the artwork and of its
148 original painting. In accordance with the Superintendence and the responsible of the Civic Museum,
149 it has been thus decided to perform a restoration aimed at recovering the original appearance of the
150 painting at the best. Consequently, in 2016 the lunette has been brought in the restoration
151 laboratories of University of Tuscia for starting the intervention.

152 The restoration work has been initially supported by traditional ultraviolet fluorescence (UVF)
153 photography aimed at mapping the superimposed materials, the grouts, the lacunae and in general
154 the non-original areas being very well visible under ultraviolet fluorescence photography. The
155 image under UV radiation showed diffuse blue fluorescence probably due to the presence of glue
156 used for the detachment of the lunette [36-37]. Grouts and cracks have been also well-highlighted by
157 the UV image [32]. Moreover, in order to characterise the blue fluorescent material visible under UV
158 radiation, Fourier transform infrared analysis was performed. This revealed that the yellowed
159 surface material was made of protein glue. The main signatures of glue have been observed in the
160 infrared spectrum at cm^{-1} : 3289, 3064, 2930, 1660, 1542, 1373, 1313, 1246, 1033 [38-39]. Other bands in
161 the spectrum have been associated to calcium carbonate (1424 and 876 cm^{-1}) and gypsum (1152 cm^{-1})

162 [32]. This preliminary analysis has been fundamental both to address the first cleaning choices of
163 restorers and to start the intervention.

164 After this, further investigations were performed by combining HMI and PuCT to obtain
165 information about the painting materials and the stratigraphic sequence, the last one being a
166 highly-inhomogeneous mix of both original layers and new grounds added during the detachment
167 of the lunette from the church of Santa Maria del Paradiso. The achieved results are illustrated in the
168 following sections, demonstrating the high potential of this integrated approach to become a
169 standard methodology in the preliminary study of the artworks to be restored.

170



171

172 **Figure 1.** The lunette with Madonna and the Child enthroned between the angels and the Saints
173 Jerome and Francis (AD 1490), attributed to the painter Antonio del Massaro known as Pastura
174 (1450-1519). The calibrated visible image with the colour checker and the white patches used for HMI
175 acquisition is shown in the figure.

176 **2. Materials and Methods**

177 2.1. Hypercolorimetric Multispectral Imaging (HMI)

178 HMI was performed through a Nikon D810FR 36 Megapixel camera, modified to obtain full
179 range spectral reflectance measurements. Nikon SB910 xenon flashes without their front plastic
180 lenses were used for lighting the painting, thus allowing the UV wavelength to be emitted as well.
181 The UVF was then obtained by filtering the flashes light with a UV band-pass filter with a spectral
182 cut at 380 nm, and UV-IR cut filter (400-700 nm) in front of the camera. The HMI image processing
183 system consists of two main software tools, i.e. SpectraPick® for the image calibration and
184 PickViewer® for the image analysis [13, 19-21, 31]. The calibration of the images was achieved by
185 placing radiometric references just below the painting. In particular, various white patches and a
186 sample with 36 patches of colour-checkers built using colour samples from the NCS – Natural
187 Colour System® catalog were placed just below the painting, see Fig.1. The spectral reflectance of
188 the references was measured in the range 220-1050 nm at *Profilocolare* laboratory, with 0.7 nm
189 accuracy (Instrument System Spectroradiometer CAS 140 CT and dark room). The calibration
190 procedure outputs a single AdobeRGB TIFF 16 bit colour image and seven monochromatic images in
191 16 bit TIFF format, containing the spectral reflectance values at 350, 450, 550, 650, 750, 850 and 950
192 nm. The last three values were used to define the IR1, IR2 and IR3 images respectively. The precision
193 achieved in the reflectance measurement across the whole 36 megapixels image is higher than 95%
194 and the colour error less than CIE2000 $\Delta E=2$ for the colour image [13]. The whole calibration and
195 alignment process require a few minutes and it can be performed in situ for an immediate results
196 analysis.

197 After the image acquisition and calibration, multispectral images were processed through the
198 HMI software PickViewer®, developed by Profilocolare. The PickViewer® software provides
199 powerful image processing tools able to reveal relevant information. Further, it allows gathering
200 information on hidden data from the images acquired with SpectraPick system, containing spectral
201 reflectance and colour coordinates for each of the 36 megapixels of the captured scene. Data are

202 calibrated and they are absolute in values, thus only depending on the spectral characteristics of the
203 surface. Several kinds of analyses are possible with PickViewer®, such as:

- 204 - adding and integrating any other imaging data (fluorescence, X-ray, thermal etc.);
- 205 - multichannel images viewer; any pixel colorimetry and spectral reflectance read-out;
- 206 - mapping by colour, spectra, arbitrary channels;
- 207 - principal components analysis (PCA);
- 208 - contrast enhancement through digital imaging processing algorithms;
- 209 - neural network based clustering;
- 210 - colour and spectral signature database;
- 211 - two ways mapping by database entry;
- 212 - any channel to RGB false colours visualization;
- 213 - channels math, indexes and normalised contrast;
- 214 - calibration and colour-checker test.

215 Each relevant result can be saved as image in TIFF, png or jpeg format. Results saved in TIFF
216 format can be reloaded as further derived channels and used combined with all the others [19].

217 2.2. *Pulse-Compression Thermography (PuCT)*

218 The experimental setup used for the PuCT is the same detailed in previous published papers,
219 wherein also an extended theoretical base of the technique can be found [32-34]. In particular, the
220 signal generation/acquisition was managed by Labview™ software. Thermograms were collected
221 through a Xenics Onca-MWIR (3.6–4.9 μm)-InSb, having a resolution of 320×240 pixels, a frame rate
222 of 40 Hz, and connected to a NI-1433 Camera Link Frame Grabber. The distance between the
223 painting and the camera was about 70 cm. Eight light emitting diode (LED) chips have been used as
224 the heat sources, each one with a maximum nominal electrical power of 50 W. Note that the LEDs
225 were not used at their maximum power — an overall electrical peak power of about 250 W was
226 reached to get the reported results. The pseudo-noise code driving the LED chips consisted in a
227 repetition of two Legendre sequences, each one of 47 bits. The duration of each bit was 1 s, thus

228 resulting in an overall excitation of 94 s. During this time, the LEDs were switched on for about half
229 of the overall excitation time, so that an overall electrical energy of ~12 kJ was delivered. Note that
230 the camera and the heating source were on the same side with respect to the inspected painting, thus
231 the PuCT was performed in reflection mode. The coded excitation voltage signal driving the LEDs
232 was provided by a TDK Lambda GEN 750W power supply. The frame grabber and the power
233 supply were synchronously driven by the signals provided by a National Instrument PCI-6711
234 Arbitrary Waveform Generator (AWG) board. Both the AWG board and the frame grabber were
235 connected to a central PC/DSP Unit.

236 A thorough description of the PuC algorithm lies beyond the scope of this work, therefore the
237 reader is referred to [28,30-31] for a deeper understanding of the whole procedure. For the sake of
238 clarity, some fundamentals aspects are worth to be here recalled:

- 239 1) For the here-employed setup, the reconstructed time trend of each pixel after the application of
240 the PuC algorithm corresponds to that achievable by exciting the sample with an equivalent
241 rectangular pulse of 1 s duration. The advantage of using PuC instead of a pulsed excitation is
242 that this fictitious single pulse carries the energy of the entire pseudo-noise Legendre sequence,
243 so that the response after PuC, and hence the thermograms, are characterized by a good
244 signal-to-noise ratio (SNR) even by using low peak power values. It must be stressed that such
245 aspect is crucial in the inspection of irreplaceable items as the artworks: while a short high-power
246 excitation pulse could damage the painting by inducing thermochromism or thermal/mechanical
247 stress, the use of a pseudo-noise excitation spread instead the energy within a longer time,
248 making the temperature rise of the sample being smooth and lower in magnitude. After PuC, a
249 fictitious larger and faster temperature increment is instead achieved exploiting the mathematical
250 properties of the coded excitation.
- 251 2) It has been shown in [31] that the use of the Hilbert transform and of the derived time-phase
252 feature from PuCT signals can help to highlight some characteristics of the support, such as the
253 wood grain, grouts, etc.. Here, the same processing is applied to the PuCT data to enhance the

254 sensitivity in the inspection of sub-surface layers. Thus, three different time-domain features will
255 be here shown. In particular: “Emissivity” — is the amplitude of the time signal of each pixel
256 retrieved after PuC and it is an indirect measure of the pixel thermal emissivity, which can be
257 related to the pixel surface temperature by a proper calibration; “Hilbert” — is the output of the
258 Hilbert transform applied pixelwise to the “Emissivity” trends; “Time-phase” — is the function
259 that for each time instant t outputs the argument of the complex number $c(t) = Emissivity(t) +$
260 $i * Hilbert(t)$ in time domain, with i being the imaginary unit.

261 3) As for HMI, PCA has been applied to the time series of thermograms produced by imaging both
262 the Emissivity and the Hilbert features. As can be seen in the next Section, PCA allows for
263 evidencing some specific characteristics of the time-series while reducing the number of images
264 to be analysed. This can be very useful for a first analysis of the sample to detect anomalies, while
265 for a quantitative analysis the processing of the image time-series is necessary.

266 4) An alternative way for presenting the thermography results has been here explored, which is
267 based on using the three abovementioned features, i.e. emissivity, Hilbert and time-phase, to
268 generate colour images. In particular, RGB, and YCbCr colour spaces have been explored by
269 relating each colour coordinate to the each of the three features.

270 As a final remark, it is important to highlight that the PuCT images showed below were obtained
271 after merging thirteen thermal acquisitions. Multiple acquisitions were performed to obtain a good
272 trade-off between the tested painting surface and the need for assuring enough spatial resolution of
273 the captured thermograms. As an example of the procedure, Figure 9a depicts the image of the
274 thermal emissivity estimated after 1 second from the beginning of the reconstructed thermal pulse.
275 Some discontinuities between the images corresponding to the various acquisitions can be seen even
276 after some preliminary image processing. Certainly, the merging procedure can be further improved
277 with a proper calibration, but this will be addressed in a next work.

278 The current results are anyway enough satisfactory to be exploited for an evaluation of the state of
279 conservation of a painting.

280 3. Results and Discussions

281 3.1. Hypercolorimetric Multispectral Imaging (HMI)

282 The seven calibrated spectral bands were analysed in PickViewer® software and some
283 processing tools were applied to the images in order to gain further diagnostic information.

284 The results of the processing are shown in Fig. 2-8. PCA was applied on IR images to highlight
285 the presence of preparatory drawing and possible *pentimenti*, especially in the restored areas where
286 different and superimposed materials are found to be highly mixed. PCA has been widely used for
287 art conservation applications, either as a stand-alone technique or to reduce the dimensionality of
288 datasets using linear algebra techniques prior to another classification algorithm whereby multiple
289 variables are analysed to evaluate the contribution of each variable to an observed result [40-41].
290 Clustering techniques can classify data based on a comparison of the spectral character of each point
291 in the image with the spectral character of every other point; this permits patterns or clusters to
292 emerge from the clustered data, thus pointing out areas of compositional similarity and returning a
293 spatial distribution of components [42].

294



295

296 **Figure 2.** The HMI infrared calibrated image at 850 nm (IR2) showing the preparatory drawing used for
 297 the construction of the painting.

298 In the detail of the foot of Saint Jerome in the IR2 image, a *pentimento* can be observed (Fig. 3) on
 299 the left side, where a different original outline was traced for drawing the foot. Figure 3 shows also
 300 the graphical user interface (GUI) of PickViewer® software: on the left an image or a selected area of
 301 the image is shown, while the processing results, according to the selected function, are visible on
 302 the right part. Extensive micro-cracking has been highlighted in correspondence of the Virgin's face
 303 by applying PCA to the images in the IR region (IR1, IR2 and IR3, see Fig. 4).

304 Another interesting processing tool of Pickviewer® is Spectral Similarities that allows for
 305 comparing the spectral reflectance of two different points on the examined surface. It was applied,
 306 for example, to the red colour in the Virgin' garment and in that of the angel at the right side of the
 307 Virgin (Fig. 5). The values of colour coordinates and of reflectance show the high similarity of the
 308 two point colour, suggesting a possible equal composition in terms of pigments.

309 In order to make hypothesis about pigment composition, especially for the blue and green ones
 310 constituting the background and the Virgin mantle, infrared false colour (IRFC) analysis has been

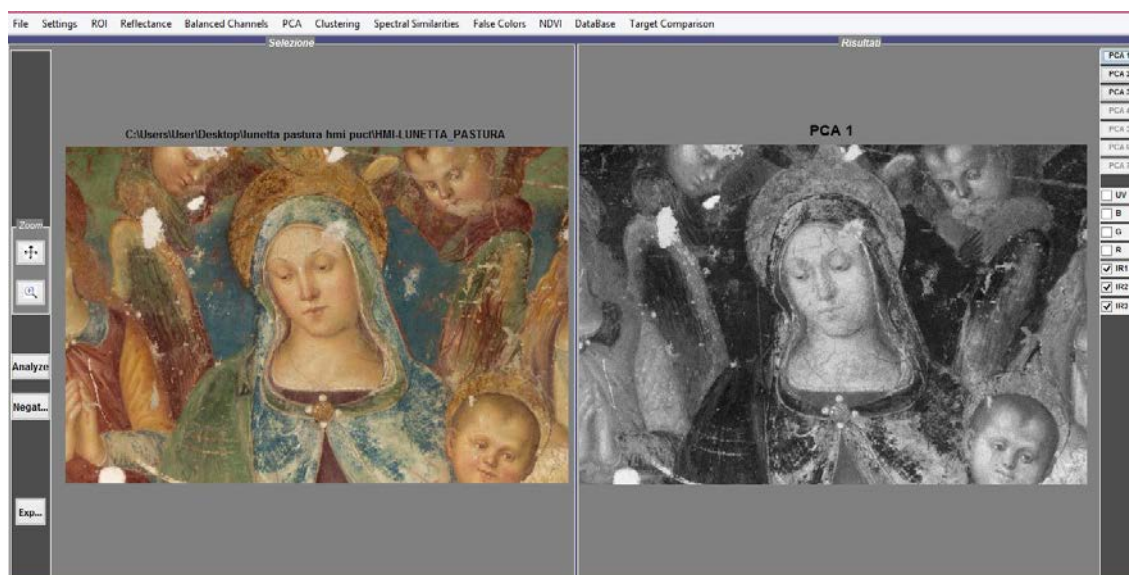
311 obtained by combining calibrated R, G, B and IR channels (Fig. 6) [43-45]. The possibility of
312 obtaining the IRFC image in a very short time by simply combining the channels, is a great
313 potentiality of PickViewer® software. For the blue pigment of the Virgin's garment, the use of azurite
314 was hypothesized on the base of its characteristic deep blue colour in IRFC. The sky and parts of the
315 vest of the Virgin have a particular green colour in the visible; in IRFC, they assume a light blue hue
316 making probable its attribution to malachite. Considering the bad state of conservation of the
317 artwork after a long exposition to weathering, a preferential degradation caused by humidity with a
318 transformation of azurite into malachite or other green copper-based compounds seems very likely,
319 rather than the application of a green pigment in areas meant to be blue-coloured [46]. Portion of
320 unaltered azurite are in fact clearly visible in the background sky behind the head of the Virgin and
321 in the lower edge of the sky as well (Fig. 7).

322



323

324 **Figure 3.** A detail of the HMI infrared calibrated image at 850 nm (IR2) showing the *pentimento* in the
325 drawing of Saint Jerome foot.

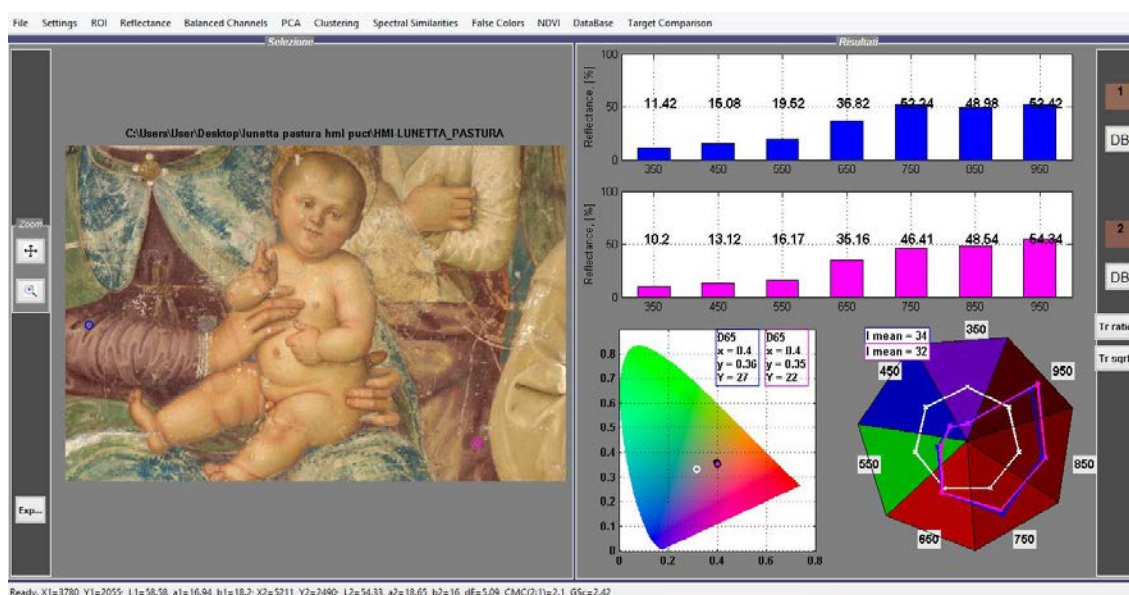


326

327

328

Figure 4. PCA applied to IR1-IR2-IR3 calibrated images showing an extensive cracking in correspondence of the Virgin's face and neck.



329

330

331

332

333

334

335

336

Figure 5. Spectral Similarities tool applied to a point on the arm of the Virgin garment and on the Angel's dress. High similarity is found both in terms of reflectance values and of colour coordinates.

In order to investigate this possibility in a non-invasive way, a map of spectral similarity was built on the base of the 7-bands curve of spectral reflectance measured in a 9×9 pixels area in the blue part of the Virgin's dress, as shown Fig. 8. The output showed on the right of the visible image in the software's GUI, highlights a correspondence between the blue pigment of the vest of the Virgin and the one used to paint the sky, supporting the hypothesis of the use of azurite in all the blue areas.

337 The painting layer of azurite used for the sky is applied over a coloured ground layer probably
338 based on red earth (hematite) or charcoal black (*morellone*), usually used for the application of azurite
339 in wall paintings, as described in scientific literature [47].

340



341

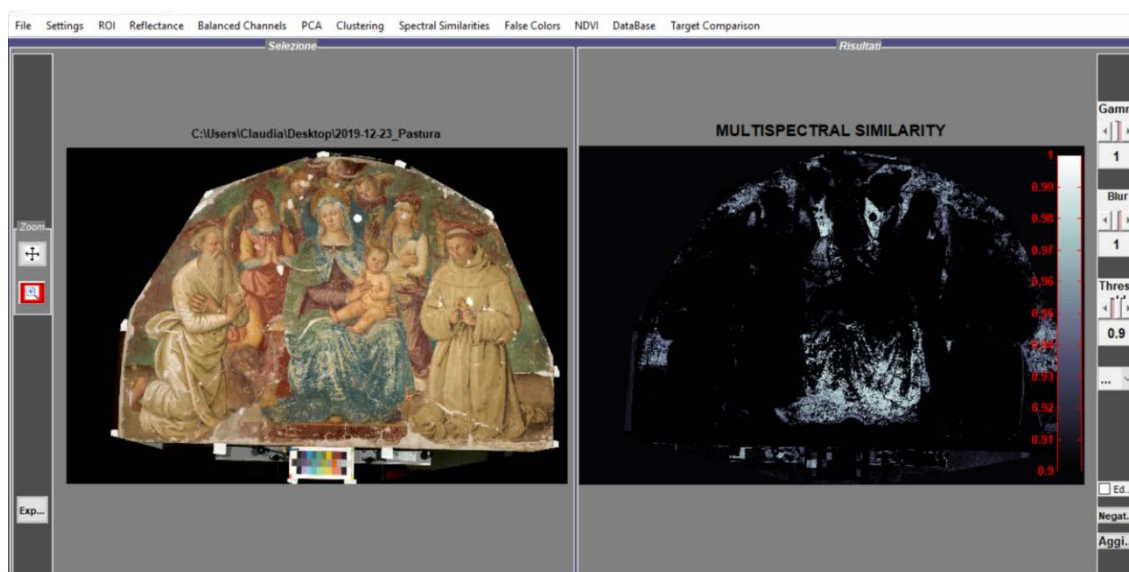
342 **Figure 6.** Infrared false colour image obtained through PickViewer®.



343

344 **Figure 7.** Detail of IRFC image showing the blue portion of the probable unaltered azurite in the
345 background sky behind the head of the Virgin.

346



347

348 **Figure 8.** Multispectral similarity mapping of azurite.

349 3.2. Pulse-Compression Thermography (PuCT)

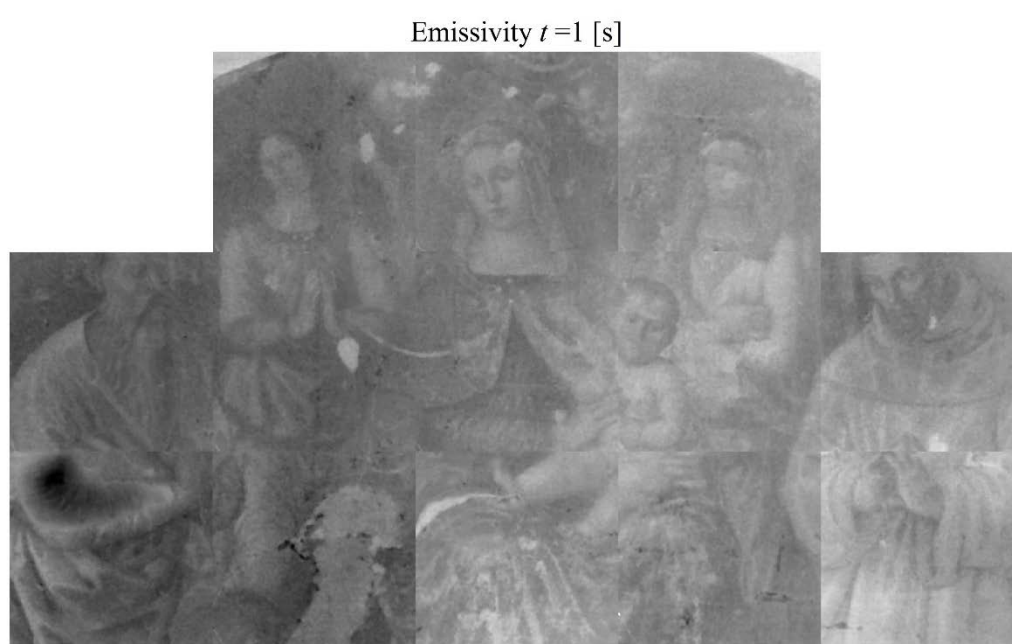
350 The reported results were obtained by applying pixelwise the Pulse-Compression (PuC)
 351 algorithm over the acquired thermograms, which has been described in detail in Sect. 2.2.

352 The IR2 band (850 nm, Fig. 2) gives some information on the preparatory drawing of the scene,
 353 as it is visible in the garments of the saints, of the angels, of the Virgin and of the lion near to Saint
 354 Jerome. Concerning the infrared PuCT analysis, the results highlight many interesting details of the
 355 surface and of the stratigraphy. Detachments, gold coating and different restoration works appear as
 356 brighter areas in emissivity images. Note that the brighter the area, the lower the emissivity. This can
 357 be seen in Fig. 9 reporting the emissivity image corresponding to $t = 1$ s, at which the fictitious
 358 excitation pulse stops, and the temperature decay starts. Typically, this is the time instant that better
 359 shows the details of the pictorial layer, since during the excitation the light is absorbed differently by
 360 the various colours, leading to a variation of the surface temperature over the sample.

361 The presence of gold traces in the haloes of the saints and angels, suggests that the haloes were
 362 originally gilded probably by using a *missione*, an adhesive oil/resin primer, used to make the
 363 adhesion of gold on the wall paintings possible [48], visible in the IRFC image with a yellow-brown
 364 colour.

365 Among the various areas of interest, the large previous restoration work between the Virgin
366 and Saint Jerome appears as a well-delimited cold area, while Saint Jerome's right arm is hotter than
367 the rest of the figure. It can be noticed that the same arm exhibits an anomalous brilliance in the IR2
368 and in false colour images (Figures 2 and 6), probably due to the use of different materials and
369 painting techniques.

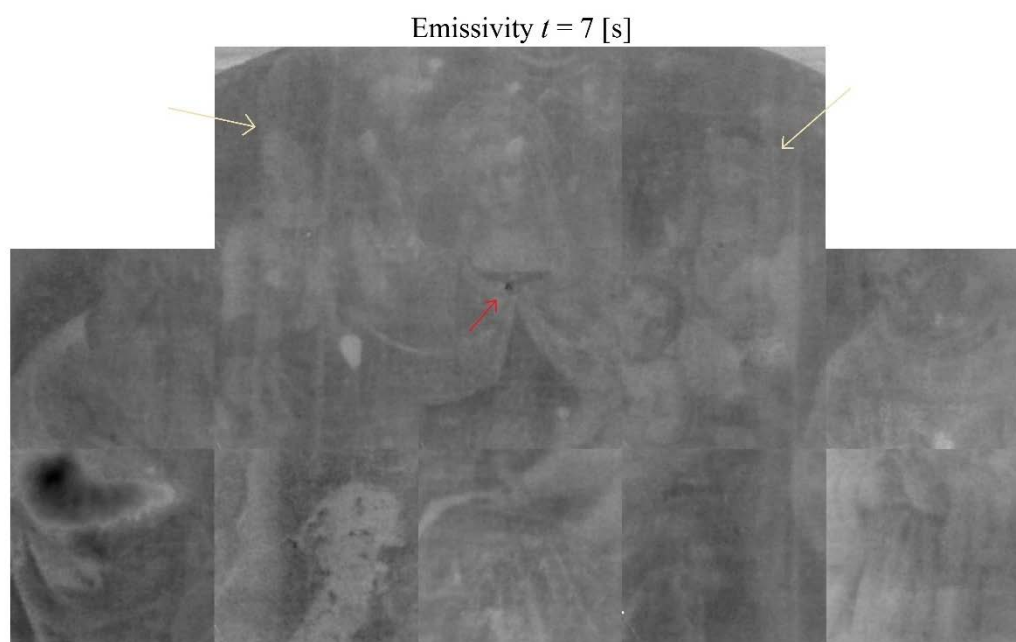
370 Then, different features become more visible as time elapses, as there is a direct link between
371 the thermal responses of layers at deeper depths within the tested materials and the flow of time.



372

373 **Figure 9.** PuCT emissivity image obtained at $t = 1$ s.

374

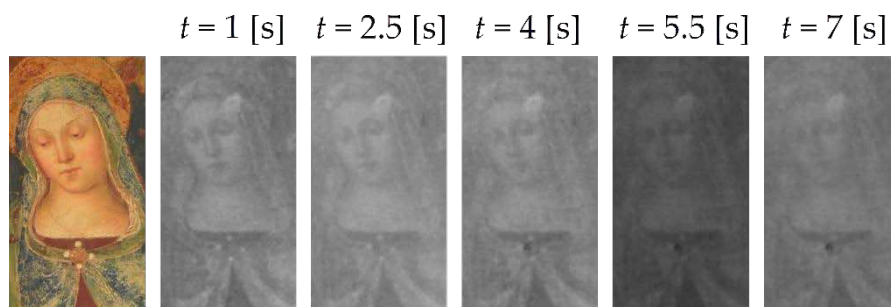


375

376 **Figure 10.** PuCT emissivity image obtained at $t = 7$ s.

377 As an example, Fig. 10 depicts the emissivity image at $t = 7$ s. Signatures of possible deeper
 378 detachments/restorations/gluing are visible as vertical contrasted areas, denoted with yellow
 379 markers. The texture of the canvas underneath the painting is also barely visible, superimposed to
 380 the faint details of the painting scene. An interesting detail concerns the Virgin's cloak closure. In
 381 Fig. 9, four lighter-colder spots are clearly visible while in Fig. 10 they are no more present but a
 382 darker-hotter spot appeared in the middle of the four previous spots. The evolution of this area in
 383 time is illustrated with more details in Fig. 11, where a zoom of this part is reported as time elapses
 384 together with the visible image serving as a reference.

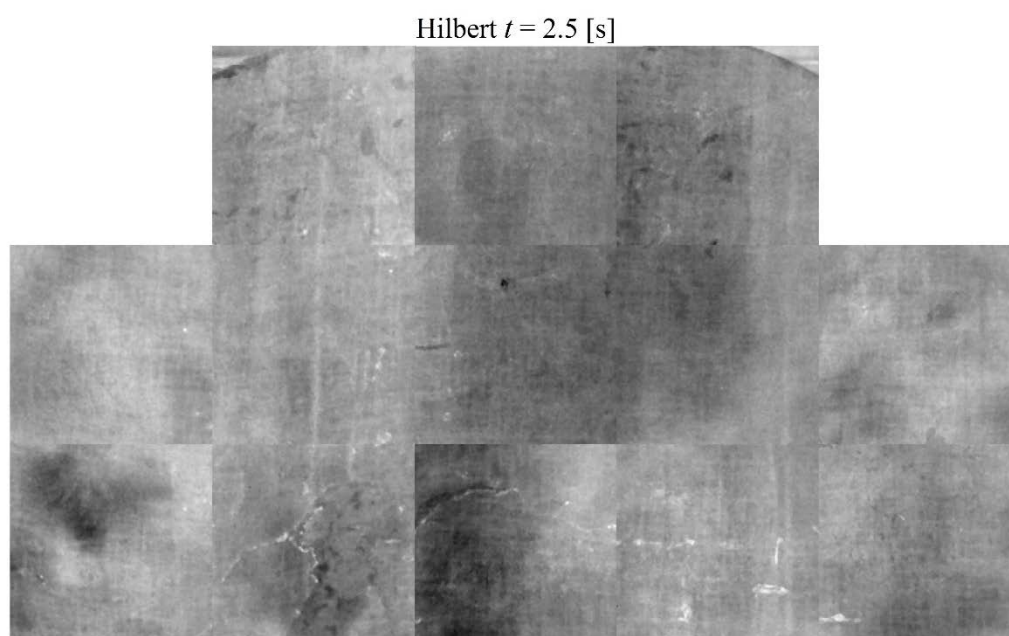
385 To better identify the support of the paintings, the images obtained by Hilbert and time-phase
 386 features can be used. Indeed, while the emissivity feature is influenced for a quite long time by the
 387 temperature rise of the pictorial layer, in the other two features, the details of the pictorial layer, i.e.
 388 the painting subject, disappears rapidly and the subsurface layers can be visualized.



389

390 **Figure 11.** PuCT emissivity images at different times representing Virgin's face and cloak closure. Darker
 391 areas corresponds to hotter areas.

392 Figure 12 shows the image of the Hilbert feature at $t = 2.5$ s, where the canvas texture — including
 393 its waviness — is clearly visible. In these thermograms, the following characteristics can be found: (i)
 394 a series of cracks, starting from the large retouching at bottom left, passing through the Virgin's
 395 knees and Child's feet; (ii) the hot spot of the cloak closure; (iii) the vertical bands and lines present
 396 also in Fig. 10; (iv) Saint Jerome's arm that appears darker/hotter; and (v) hot and cold spots
 397 scattered all around the painting.



398

399 **Figure 12.** PuCT Hilbert image obtained at $t = 2.5$ s.

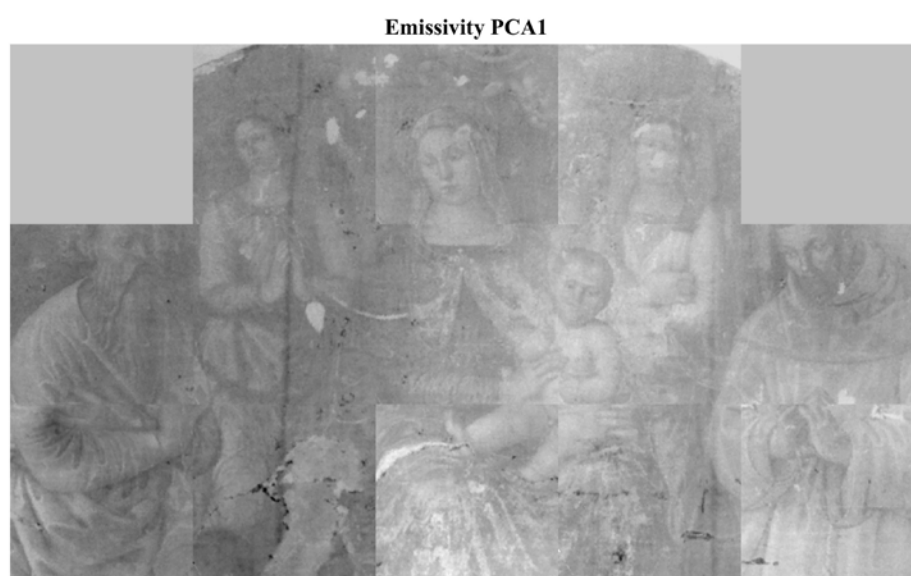
400

401 Other frames corresponding to different time instants could be selected to better highlight
 402 different details, but the main aim is here to demonstrate the capability of the PuCT technique to

403 provide information from the inner structure of the sample to be complemented by HMI
404 information.

405 PCA can be applied separately to emissivity, Hilbert and time-phase images, or to all the
406 images together. It has been found that the application of PCA to the emissivity time series only
407 allows most of the details of interest to be visualized in a few images, as it can be seen in Figures 13
408 to 15 showing the first three PCA components. In particular, the PCA3 image in Fig. 15 depicts the
409 canvas under the painting, even if these were not so appreciable in the emissivity images.

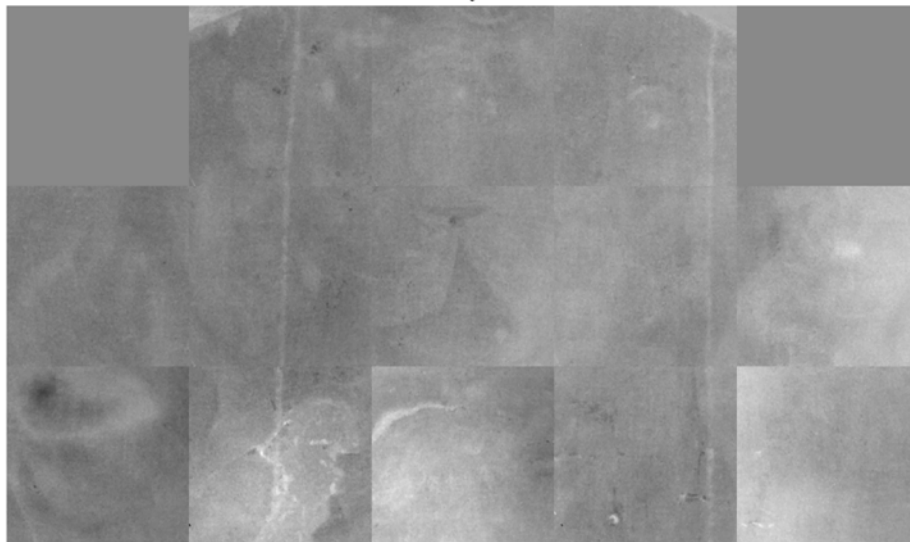
410 As a further investigation, the data reported in Figs. 13-15 have been transformed from the grey
411 scale to the YCbCr colour space [49]. This is because the human eye have a different perception
412 between a grey scale image and its coloured replica, thus this can help in highlighting areas having
413 different thermal contrasts. Although the perception is inherently highly subjective by nature and
414 further investigation are needed to confirm the validity of the proposed approach — including the
415 possibility to submit a survey to several experts in the field — in our opinion, Figs. 16-18 shows an
416 enhanced perception of the abovementioned area of interests with respect to the same depicted in
417 Figs. 13-15.



418

419 **Figure 13.** First PCA image retrieved by PuCT emissivity time series image.

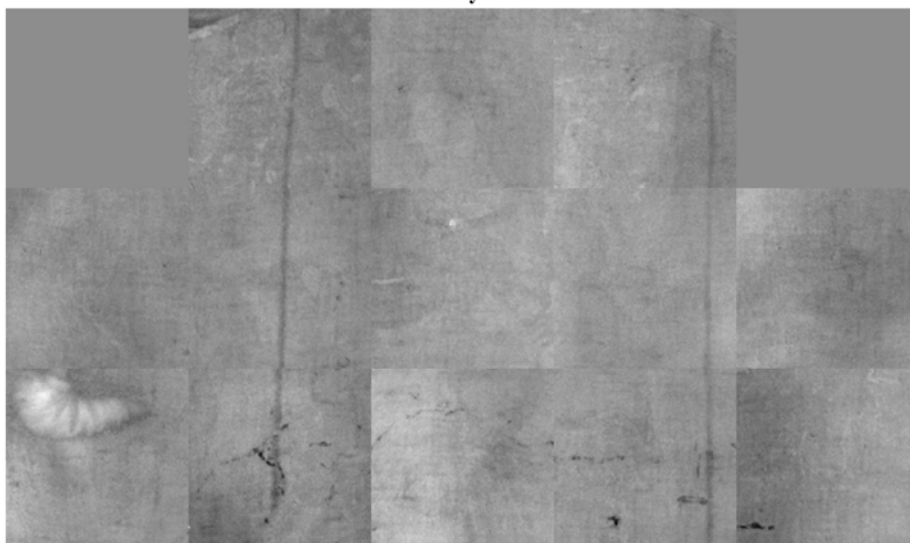
Emissivity PCA2



420

421 **Figure 14.** Second PCA image retrieved by PuCT emissivity time series image.

Emissivity PCA3

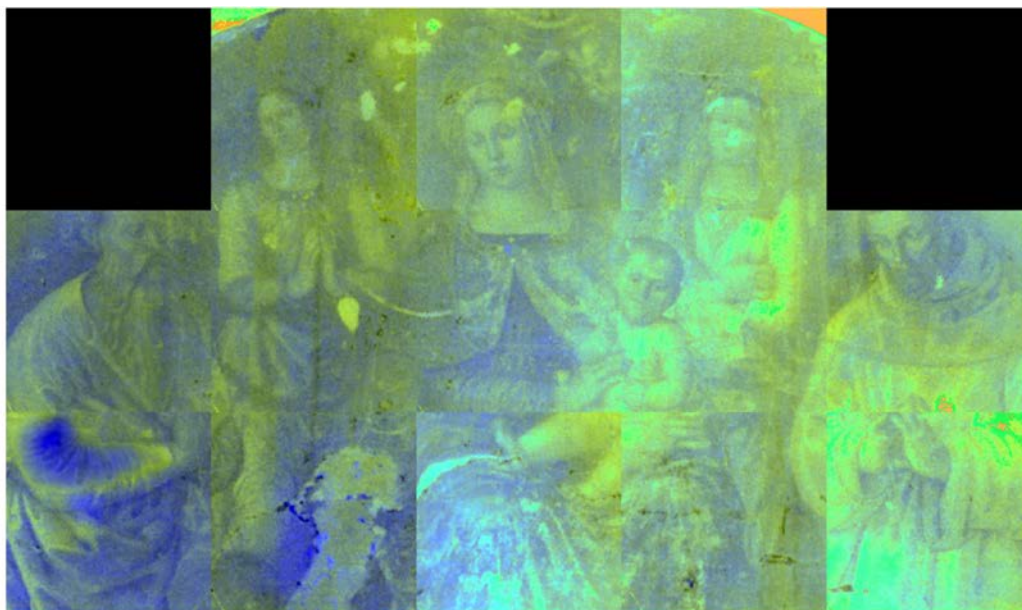


422

423 **Figure 15.** Third PCA image retrieved by PuCT emissivity time series image.

424

425

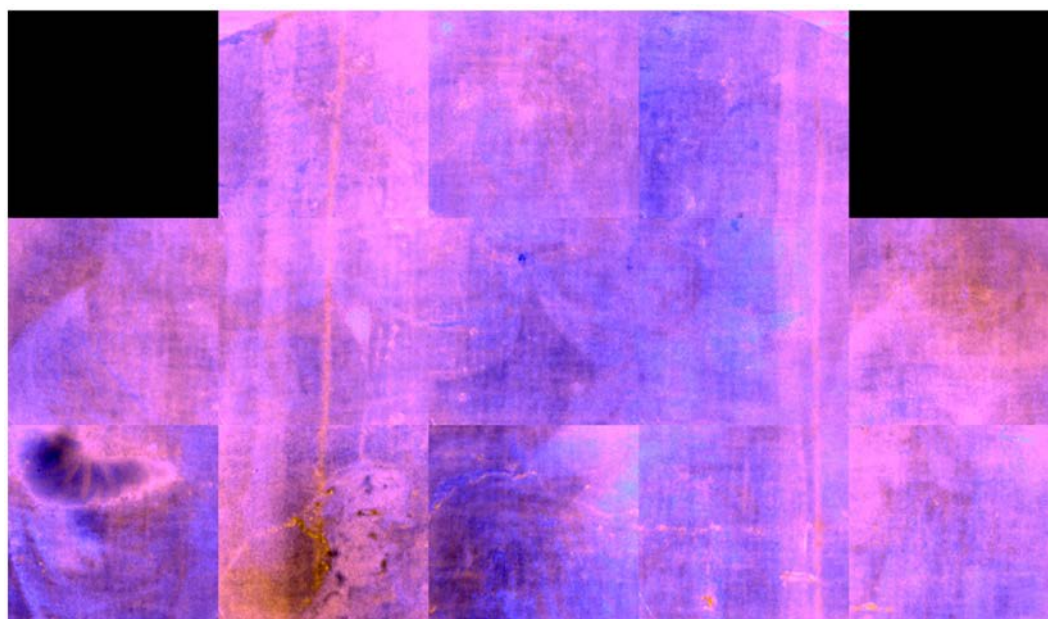


426

427

428

Figure 16. False-colour PuCT – YCbCr colour space at $t=1$ s PCA image retrieved by PuCT emissivity time series image.



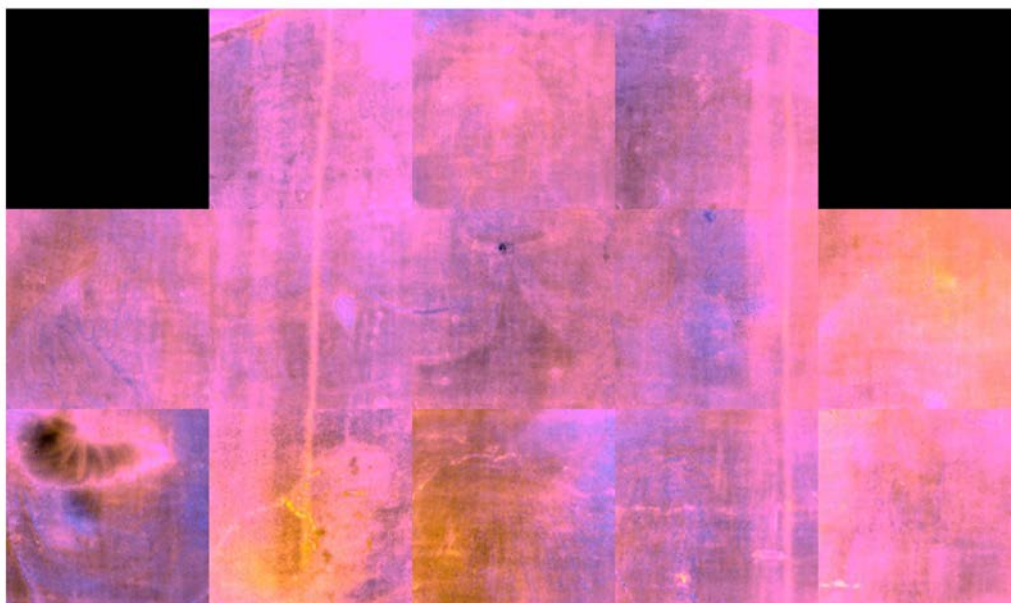
429

430

431

432

Figure 17. False-colour PuCT – YCbCr colour space at $t=3$ s PCA image retrieved by PuCT emissivity time series image.



433

434 **Figure 18.** False-colour PuCT – YCbCr colour space at $t=4$ s PCA image retrieved by PuCT emissivity time
 435 series image.

436 5. Conclusions

437 Hypercolorimetric Multispectral Imaging (HMI) and Pulse-Compression Thermography
 438 (PuCT) have been tested on a detached wall painting representing the Madonna and the Child
 439 enthroned between the angels and the Saints Jerome and Francis (AD 1490), attributed to the painter
 440 Antonio del Massaro known as Pastura (1450-1519).

441 The combined use of the two techniques, for the first time on a wall painting, was possible
 442 thanks to the restoration work, offering the chance for investigating the artwork to study the
 443 materials, the construction techniques, the state of preservation and the stratigraphic pattern as
 444 consequence of the detachment operations performed at the beginning of the 20th century.

445 HMI supplied relevant information about surface and sub-surface layers in terms of possible
 446 pigment composition and distribution, and preparatory drawing/*pentimenti*, respectively.

447 PuCT output signatures of detachments, grouting, gilding from the surface to the deep layers
 448 giving relevant information about the possible presence of discontinuity or deep grouts. A color
 449 space transformation from gray scale to YCbCr was found to be useful for highlighting areas of
 450 interest.

451 Further processing of the acquired images will be possible also with the support of conservators
 452 that could address the choice of the most useful deepening to supply a valid aid to the intervention.

453 6. Declarations

454 **Availability of Data and Material:** The datasets used and/or analysed during the current study are available
 455 from the corresponding author on reasonable request.

456 **Competing Interest:** The authors declare no competing of interest.

457 **Funding:** This research received no external funding

458 **Author Contributions:** Conceptualization, M.R., M.M., S.S., S.L., G.C. and C.P.; methodology, M.R., S.S., M.M.,
 459 C.P. and S.L.; software, S.L., M.R., M.M.; validation, S.L., M.R., M.M. and H.M; formal analysis, S.L., M.R., G.A.,
 460 L.L., C.C. and H.M; investigation, M.R., S.L., G.A., L.L., C.C. and H.M; resources, G.C., M.R., S.S. and C.P.; data
 461 curation, M.R., C.P., S.L., C.C. and H.M; writing—original draft preparation, C.P. and M.R.; writing—review
 462 and editing, S.L. and H.M; visualization, C.C., M.R., G.A., L.L. and S.L.; supervision, G.C. and M.R.; project
 463 administration, M.R. and G.C.; funding acquisition, M.R., S.S., G.C. and C.P. All authors have read and agreed
 464 to the published version of the manuscript.

465 **Acknowledgments:** Authors would like to thank the restorer Dr. Mark Gittins and the art historian Dr. Paola
 466 Pogliani teachers in the LMR/02 course for having allowed us to perform the investigation of the lunette. The
 467 authors acknowledge fruitful discussions with Dr. Saverio Ricci about the history of the artwork inspected.

468 List of abbreviations:

HMI	Hypcolorimetric multispectral imaging
PuCT	Pulse-compression thermography
CH	Cultural heritage
MS	Multispectral
HS	Hyperspectral
UV	Ultraviolet
VIS	Visible
IR	Infrared
TTR	Terahertz time resolved
OCT	Optical coherence tomography
IRT	Infrared thermography
UVF	Ultraviolet fluorescence
LED	Light emitting diode
AWG	Arbitrary waveform generator
PCA	Principal component analysis
SNR	Signal-to-noise ratio

PuC Pulse-compression
 GUI Graphical user interface
 IRFC Infrared false colour

469

470 **References**

- 471 1. Aldrovandi A, Bertani D, Cetica M, Matteini M, Moles A, Poggi P, Tiano P. Multispectral image processing
 472 of paintings. *Studies in Conservation*. 1988 Aug 1;33(3):154-9.
- 473 2. Mairinger F. UV-, IR-and X-ray imaging. Non-destructive microanalysis of cultural heritage materials.
 474 2004 Jan 1;42:15-73.
- 475 3. Saunders D, Billinge R, Cupitt J, Atkinson N, Liang H. A new camera for high-resolution infrared imaging
 476 of works of art. *Studies in conservation*. 2006 Jan 1;51(4):277-90.
- 477 4. Fischer C, Kakoulli I. Multispectral and hyperspectral imaging technologies in conservation: current
 478 research and potential applications. *Studies in Conservation*. 2006 Jun 1;51(sup1):3-16.
- 479 5. Kubik M. Hyperspectral imaging: a new technique for the non-invasive study of artworks. *Physical*
 480 *techniques in the study of art, archaeology and cultural heritage*. 2007 Jan 1;2:199-259.
- 481 6. Delaney JK, Zeibel JG, Thoury M, Littleton RO, Palmer M, Morales KM, de La Rie ER, Hoenigswald AN.
 482 Visible and infrared imaging spectroscopy of Picasso's Harlequin musician: mapping and identification of
 483 artist materials in situ. *Applied spectroscopy*. 2010 Jun 1;64(6):584-94.
- 484 7. Adam AJ, Planken PC, Meloni S, Dik J. Terahertz imaging of hidden paint layers on canvas. *Optics*
 485 *Express*. 2009 Mar 2;17(5):3407-16.
- 486 8. Fukunaga K, Picollo M. Terahertz spectroscopy applied to the analysis of artists' materials. *Applied*
 487 *Physics A*. 2010 Sep 1;100(3):591-7.
- 488 9. Casini A, Bacci M, Cucci C, Lotti F, Porcinai S, Picollo M, Radicati B, Poggese M, Stefani L. Fiber optic
 489 reflectance spectroscopy and hyper-spectral image spectroscopy: two integrated techniques for the study
 490 of the Madonna dei Fusi. In *Optical methods for arts and archaeology 2005 Aug 12 (Vol. 5857, p. 58570M)*.
 491 International Society for Optics and Photonics.
- 492 10. Elias M, Mas N, Cotte P. Review of several optical non-destructive analyses of an easel painting.
 493 Complementarity and crosschecking of the results. *Journal of cultural heritage*. 2011 Oct 1;12(4):335-45.
- 494 11. Luciani G, Pelosi C, Agresti G, Lo Monaco A. How to reveal the invisible the fundamental role of
 495 diagnostics for religious painting investigation. *Eur. J. Sci. Theol*. 2019 Jun;15:209-20.

- 496 12. Lanteri L, Agresti G, Pelosi C. A new practical approach for 3D documentation in ultraviolet fluorescence
497 and infrared reflectography of polychromatic sculptures as fundamental step in restoration. *Heritage*.
498 2019 Mar;2(1):207-15.
- 499 13. Colantonio C, Pelosi C, D'Alessandro L, Sottile S, Calabrò G, Melis M. Hypercolorimetric multispectral
500 imaging system for cultural heritage diagnostics: an innovative study for copper painting examination.
501 *The European Physical Journal Plus*. 2018 Dec 1;133(12):526.
- 502 14. Pelosi C, Calienno L, Fodaro D, Borrelli E, Rubino AR, Sforzini L, Lo Monaco A. An integrated approach to
503 the conservation of a wooden sculpture representing Saint Joseph by the workshop of Ignaz Günther
504 (1727–1775): analysis, laser cleaning and 3D documentation. *Journal of Cultural Heritage*. 2016 Jan
505 1;17:114-22.
- 506 15. Lo Monaco A, Giagnacovo C, Falcucci C, Pelosi C. The triptych of the Holy Saviour in the Tivoli Cathedral:
507 diagnosis, conservation and religious requirements. *European Journal of Science and Theology*. 2015 Apr
508 1;11(2):241-52.
- 509 16. Pelosi C, Falcucci C, Ardagna V. Investigation of a medieval illuminated manuscript through non-invasive
510 techniques. *European Journal of Science and Theology*. 2017 Apr 1;13(2):61-8.
- 511 17. Laureti S, Malekmohammadi H, Rizwan MK, Burrascano P, Sfarra S, Mostacci M, Ricci M. Looking
512 through paintings by combining hyper-spectral imaging and pulse-compression thermography. *Sensors*.
513 2019 Jan;19(19):4335.
- 514 18. Rosi F, Miliani C, Braun R, Harig R, Sali D, Brunetti BG, Sgamellotti A. Noninvasive analysis of paintings
515 by mid-infrared hyperspectral imaging. *Angewante Chemie* 2013; 52:1-5.
- 516 19. Melis M, Miccoli M, Quarta D. Multispectral hypercolorimetry and automatic guided pigment
517 identification: some masterpieces case studies. In *Optics for arts, architecture, and archaeology IV 2013*
518 May 30 (Vol. 8790, p. 87900W). International Society for Optics and Photonics.
- 519 20. Samadelli M, Melis M, Miccoli M, Vigl EE, Zink AR. Complete mapping of the tattoos of the 5300-year-old
520 Tyrolean Iceman. *Journal of Cultural Heritage*. 2015 Sep 1;16(5):753-8.
- 521 21. Melis M, Miccoli M. Trasformazione evolutivistica di una fotocamera reflex digitale in un sofisticato
522 strumento per misure fotometriche e colorimetriche. *Proc. Colore e Colorimetria contributi multidisciplinari*;
523 RN, Italy, 2013; Vol. IXA, pp. 28-38.

- 524 22. Dong J, Locquet A, Melis M, Citrin DS. Global mapping of stratigraphy of an old-master painting using
525 sparsity-based terahertz reflectometry. *Scientific reports*. 2017 Nov 8;7(1):1-2.
- 526 23. Alberghina MF, Macchia A, Capizzi P, Schiavone S, Ruffolo SA, Comite V, Barberio M, La Russa MF.
527 Surface and volume non-invasive methods for the structural monitoring of the bass-relief 'Madonna con
528 Bambino'(Gorizia, Northern Italy). *Natural product research*. 2019 Apr 3;33(7):1034-9.
- 529 24. Elkhuizen WS, Callewaert TW, Leonhardt E, Vandivere A, Song Y, Pont SC, Geraedts JM, Dik J.
530 Comparison of three 3D scanning techniques for paintings, as applied to Vermeer's 'Girl with a Pearl
531 Earring'. *Heritage Science*. 2019 Dec 1;7(1):89.
- 532 25. Zhang H, Sfarra S, Saluja K, Peeters J, Fleuret J, Duan Y, Fernandes H, Avdelidis N, Ibarra-Castanedo C,
533 Maldague X. Non-destructive investigation of paintings on canvas by continuous wave terahertz imaging
534 and flash thermography. *Journal of Nondestructive Evaluation*. 2017 Jun 1;36(2):34.
- 535 26. Maldague X. *Theory and practice of infrared thermography for nondestructive testing*. Wiley series in microwave
536 and optical engineering. Wiley: Hoboken NJ, USA, 2001.
- 537 27. Bodnar JL, Nicolas JL, Candoré JC, Detalle V. Non-destructive testing by infrared thermography under
538 random excitation and ARMA analysis. *International Journal of Thermophysics*. 2012 Nov
539 1;33(10-11):2011-5.
- 540 28. Silipigni G, Burrascano P, Hutchins DA, Laureti S, Petrucci R, Senni L, Torre L, Ricci M. Optimization of
541 the pulse-compression technique applied to the infrared thermography nondestructive evaluation. *NDT &
542 E International*. 2017 Apr 1;87:100-10.
- 543 29. Laureti S, Sfarra S, Malekmohammadi H, Burrascano P, Hutchins DA, Senni L, Silipigni G, Maldague XP,
544 Ricci M. The use of pulse-compression thermography for detecting defects in paintings. *Ndt & E
545 International*. 2018 Sep 1;98:147-54.
- 546 30. Sfarra S, Laureti S, Gargiulo G, Malekmohammadi H, Sangiovanni MA, La Russa M, Burrascano P, Ricci
547 M. Low Thermal Conductivity Materials and Very Low Heat Power: A Demanding Challenge in the
548 Detection of Flaws in Multi-Layer Wooden Cultural Heritage Objects Solved by Pulse-Compression
549 Thermography Technique. *Applied Sciences*. 2020 Jan;10(12):4233.
- 550 31. Laureti S, Colantonio C, Burrascano P, Melis M, Calabrò G, Malekmohammadi H, Sfarra S, Ricci M, Pelosi
551 C. Development of integrated innovative techniques for paintings examination: The case studies of The

- 552 Resurrection of Christ attributed to Andrea Mantegna and the Crucifixion of Viterbo attributed to
553 Michelangelo's workshop. *Journal of Cultural Heritage*. 2019 Nov 1;40:1-6.
- 554 32. Gittins M, Agresti G, Catalano MI, Pelosi C, Pogliani P. La lunette raffigurante Madonna con Bambino in
555 trono tra gli angeli e i Santi Francesco e Girolamo staccato dal convento di Santa Maria del Paradiso per il
556 Museo Civico di Viterbo: fortuna dell'opera e storia conservativa alla luce dell'ultimo restauro (2016-2017).
557 In *Proc. XV Congresso Nazionale IGIC Lo Stato dell'Arte*. Firenze, Italy, 2017; pp. 461-468.
- 558 33. Ricci C. *Antonio da Viterbo detto il Pastura e l'Appartamento Borgia. Per l'inaugurazione del Museo Civico di*
559 *Viterbo*. Agnesotti: Viterbo, Italy, 1912; pp. 23-27.
- 560 34. Zuccari A. L'attività viterbese di Antonio del Massaro detto il Pastura. *Il Quattrocento a Viterbo*. Milano,
561 1983; pp. 222-239.
- 562 35. Rinaldi S. *I dipinti del Museo Civico di Viterbo. Censimento conservativo in omaggio a Michele Cordaro*. Ediart:
563 Tody, Italy, 2004; p. 75.
- 564 36. Pelosi C, Lanteri L, Agresti G, Santamaria U. Documentation and Scientific Investigation on the
565 "Crucifixion" by Balletta in the church of Santa Maria Nova in Viterbo (Italy). *Conservation and Religious*
566 *Requirements*. *European Journal of Science and Theology*. 2016 Feb;12(1):271-81.
- 567 37. Lanteri L, Agresti G. Ultraviolet fluorescence 3D models for diagnostics of cultural heritage. *Eur. J. Sci.*
568 *Theol*. 2017 Apr 1;13:35-40.
- 569 38. Derrick MR, Stulik D, Landry JM. *Infrared spectroscopy in conservation science*. Getty Publications; 2000
570 Mar 16.
- 571 39. Meilunas RJ, Bentsen JG, Steinberg A. Analysis of aged paint binders by FTIR spectroscopy. *Studies in*
572 *conservation*. 1990 Feb 1;35(1):33-51.
- 573 40. Bro R, Smilde AK. Principal component analysis. *Analytical Methods*. 2014;6(9):2812-31.
- 574 41. Pelosi C, Capobianco G, Agresti G, Bonifazi G, Morresi F, Rossi S, Santamaria U, Serranti S. A
575 methodological approach to study the stability of selected watercolours for painting reintegration,
576 through reflectance spectrophotometry, Fourier transform infrared spectroscopy and hyperspectral
577 imaging. *Spectrochimica Acta Part A: Molecular and Biomolecular Spectroscopy*. 2018 Jun 5;198:92-106.
- 578 42. Lau D, Villis C, Furman S, Livett M. Multispectral and hyperspectral image analysis of elemental and
579 micro-Raman maps of cross-sections from a 16th century painting. *Analytica chimica acta*. 2008 Mar
580 3;610(1):15-24.

- 581 43. Cosentino A. Infrared technical photography for art examination. *e-Preservation Science*. 2016;13:1-6.
- 582 44. Cosentino A. Identification of pigments by multispectral imaging; a flowchart method. *Heritage Science*.
583 2014 Dec 1;2(1):8.
- 584 45. Cosentino A. Effects of different binderson technical photography and reflectography of 54 historical
585 pigments. *International Journal of Conservation Science*. 2015 Sep 1;6(3).
- 586 46. Cavallo G. Alteration of azurite into paratacamite at the St. Alessandro church (Lasnigo, Italy). *Conservar*
587 *património*. 2009(9):5-11.
- 588 47. Sandu IC, Afonso LU, Murta E, de Sa MH. Gilding techniques in religious art between east and west,
589 14th-18th centuries. *International Journal of Conservation Science*. 2010 Mar;1(1):47-62.
- 590 48. Sandu IC, Afonso LU, Murta E, de Sa MH. Gilding techniques in religious art between east and west,
591 14th-18th centuries. *International Journal of Conservation Science*. 2010 Mar;1(1):47-62.
- 592 49. Liu C, van Netten JJ., Van Baal JG, Bus SA, van Der Heijden F. Automatic detection of diabetic foot
593 complications with infrared thermography by asymmetric analysis. *Journal of biomedical optics*.
594 2015; 20(2), 026003.

© 2020 by the authors. Submitted for possible open access publication under the terms



and conditions of the Creative Commons Attribution (CC BY) license

(<http://creativecommons.org/licenses/by/4.0/>).

Figures



Figure 1

The lunette with Madonna and the Child enthroned between the angels and the Saints Jerome and Francis (AD 1490), attributed to the painter Antonio del Massaro known as Pastura (1450-1519). The calibrated visible image with the colour checker and the white patches used for HMI acquisition is shown in the figure.



Figure 2

The HMI infrared calibrated image at 850 nm (IR2) showing the preparatory drawing used for the construction of the painting.



Figure 3

A detail of the HMI infrared calibrated image at 850 nm (IR2) showing the pentimento in the drawing of Saint Jerome foot.

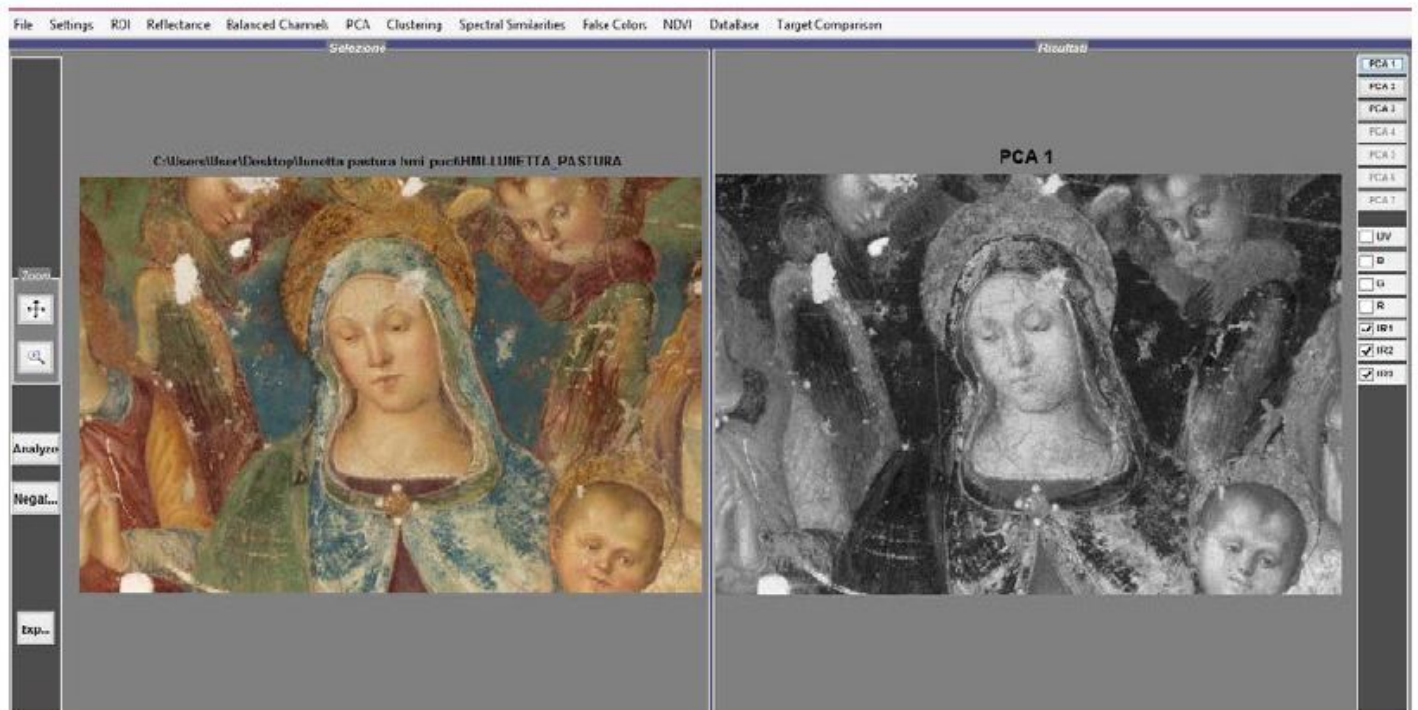


Figure 4

PCA applied to IR1-IR2-IR3 calibrated images showing an extensive cracking in correspondence of the Virgin's face and neck.

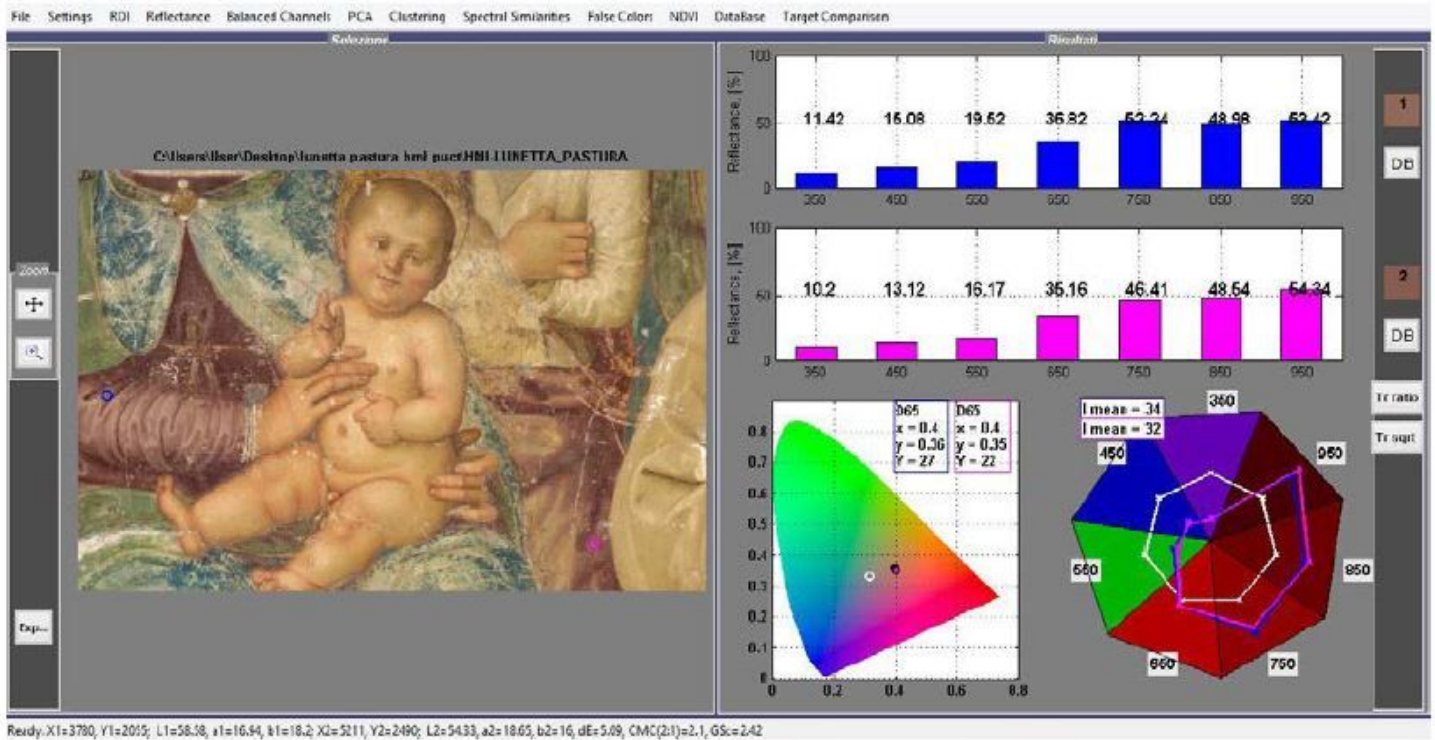


Figure 5

Spectral Similarities tool applied to a point on the arm of the Virgin garment and on the Angel's dress. High similarity is found both in terms of reflectance values and of colour coordinates.



Figure 6

Infrared false colour image obtained through PickViewer®.



Figure 7

Detail of IRFC image showing the blue portion of the probable unaltered azurite in the background sky behind the head of the Virgin.

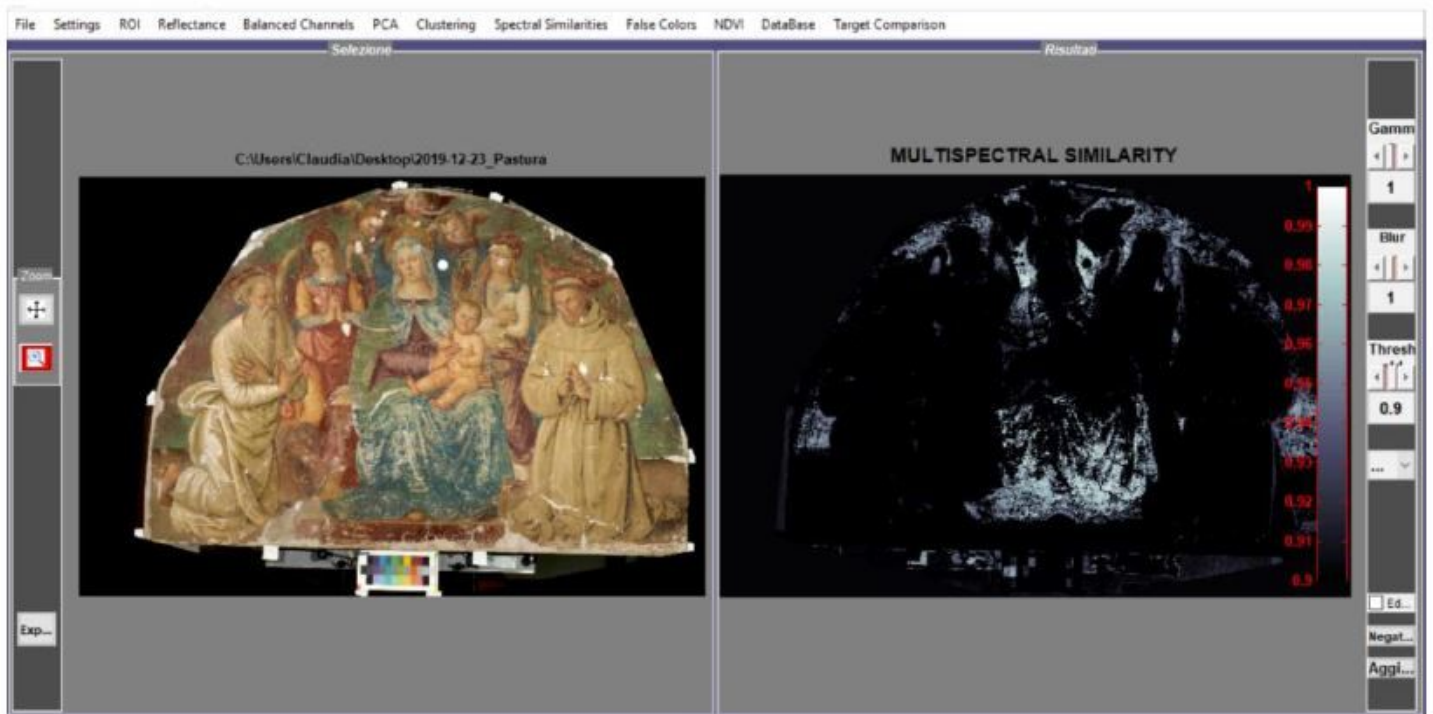


Figure 8

Multispectral similarity mapping of azurite.

Emissivity $t = 1$ [s]



Figure 9

PuCT emissivity image obtained at $t = 1$ s.

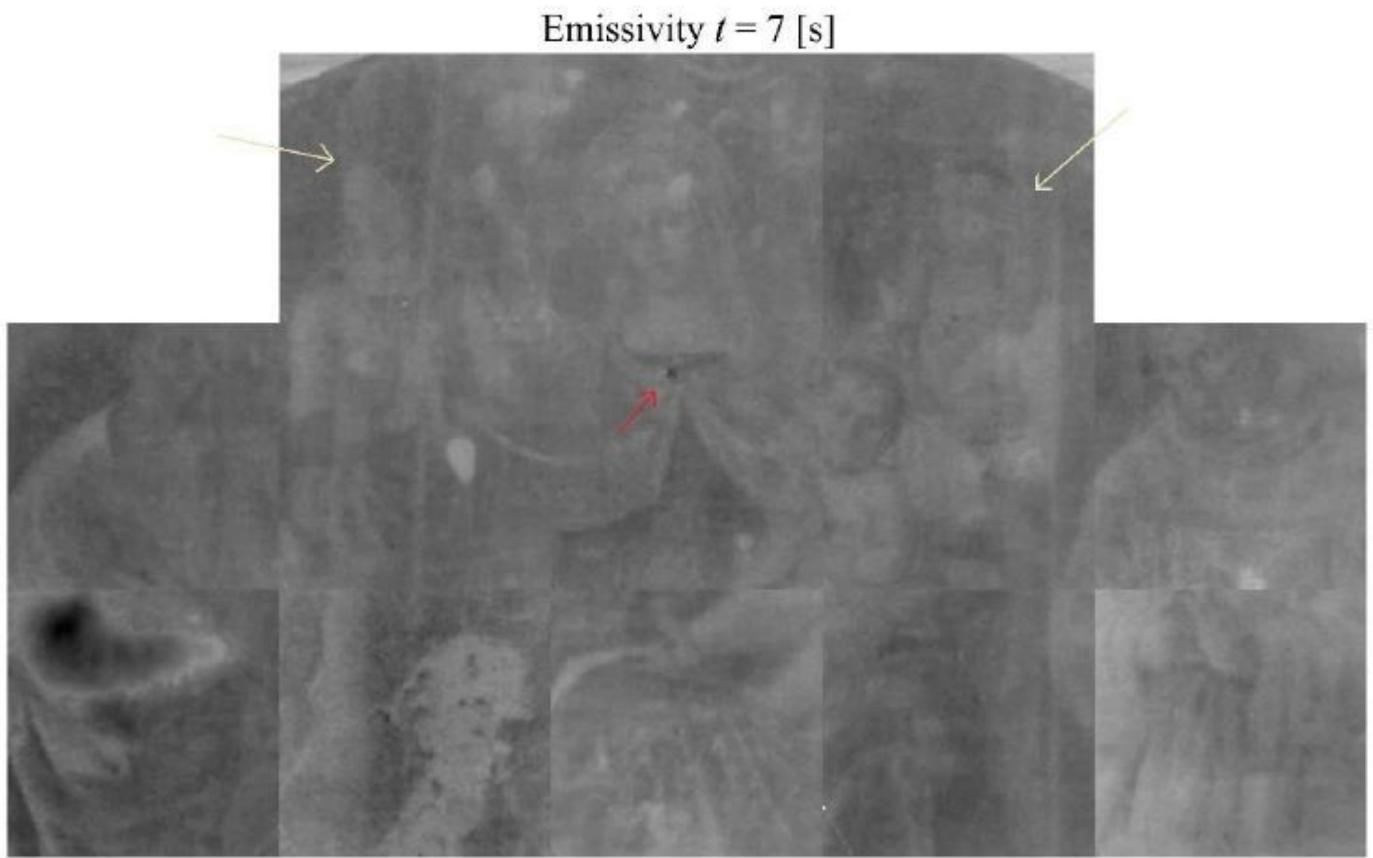


Figure 10

PuCT emissivity image obtained at $t=7$ s.

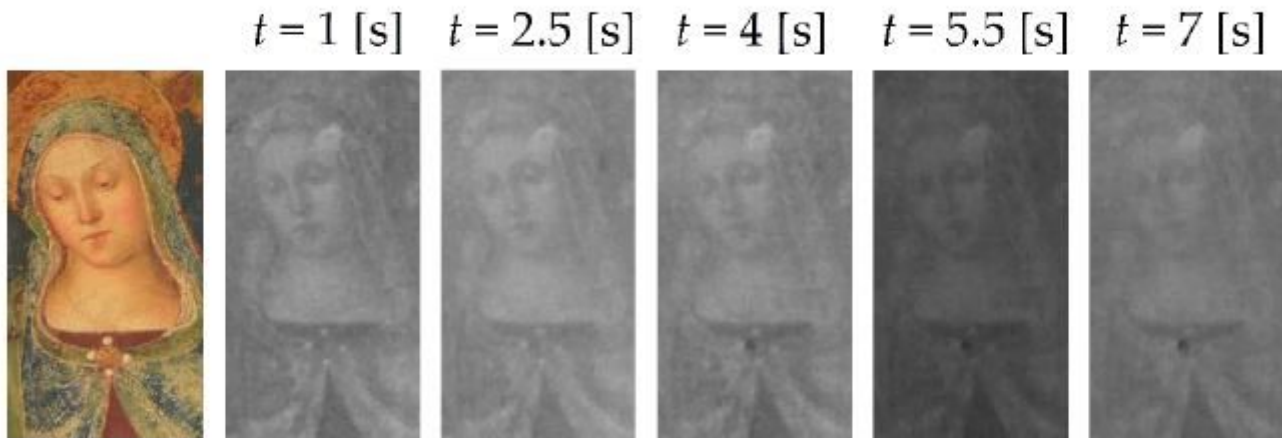


Figure 11

PuCT emissivity images at different times representing Virgin's face and cloak closure. Darker areas corresponds to hotter areas.

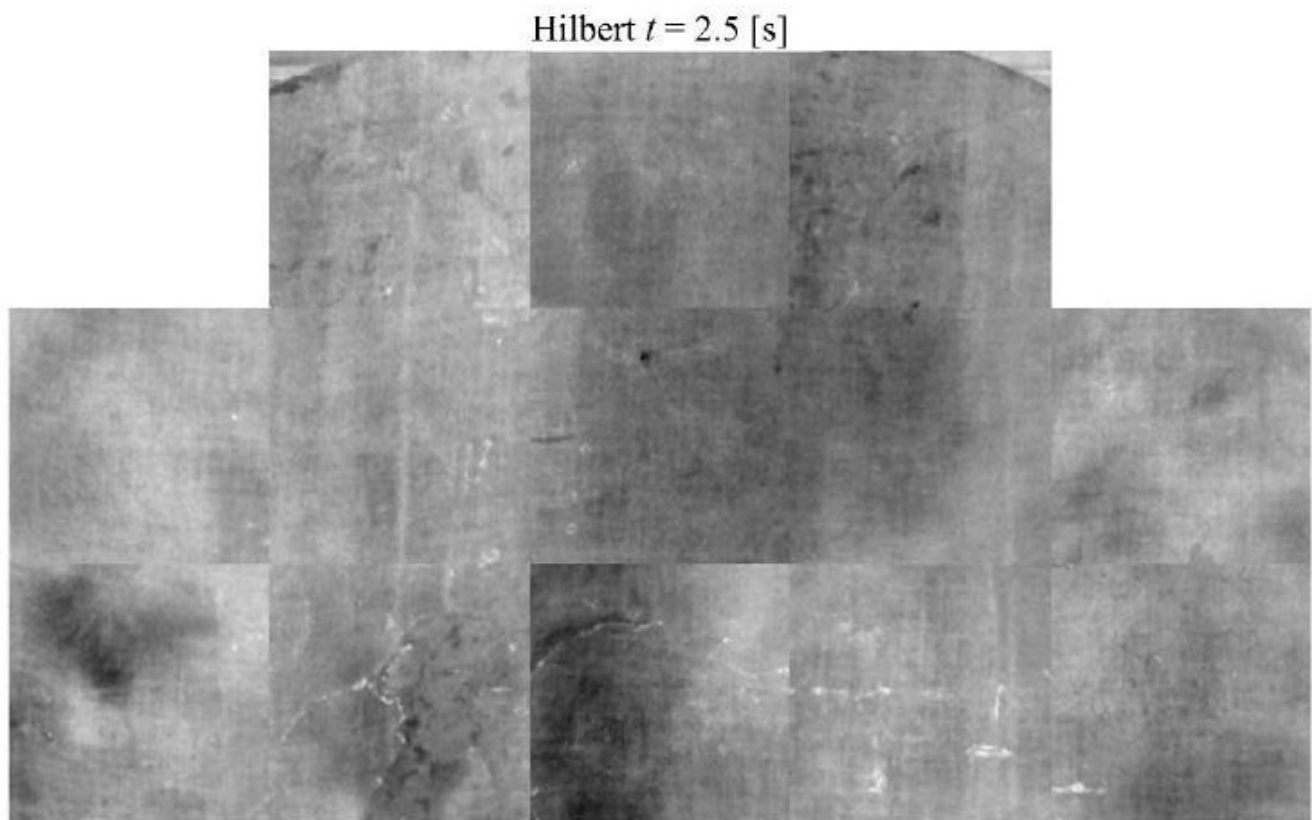


Figure 12

PuCT Hilbert image obtained at $t=2.5$ s.

Emissivity PCA1



Figure 13

First PCA image retrieved by PuCT emissivity time series image.

Emissivity PCA2

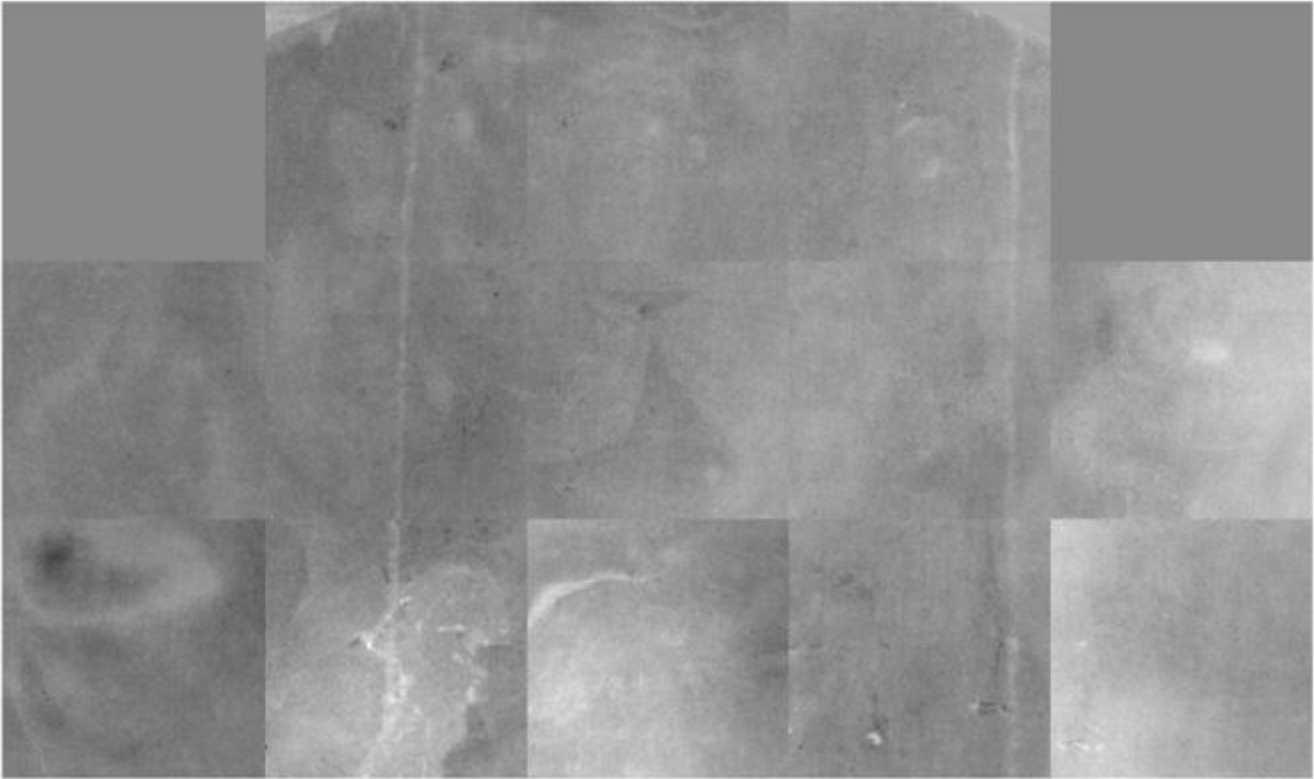


Figure 14

Second PCA image retrieved by PuCT emissivity time series image.

Emissivity PCA3

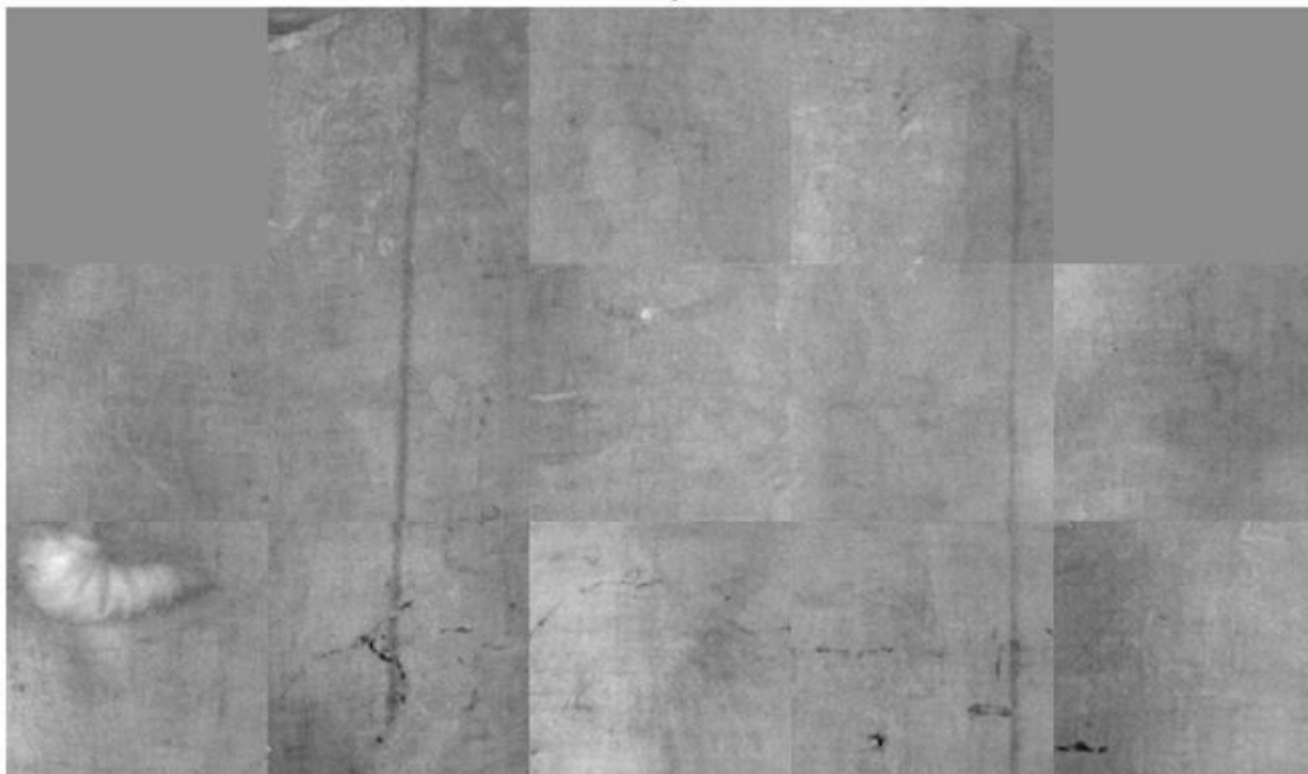


Figure 15

Third PCA image retrieved by PuCT emissivity time series image.

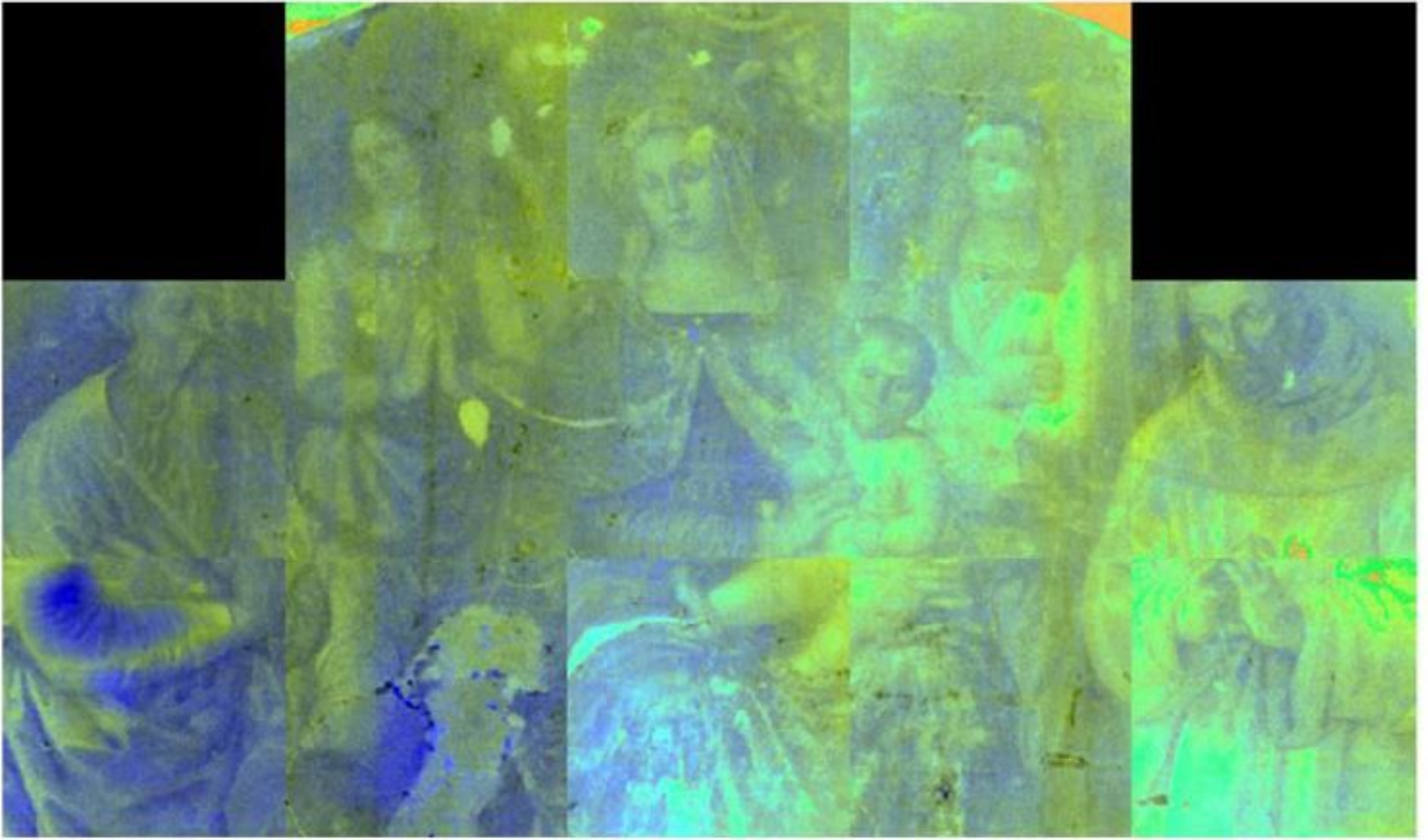


Figure 16

False-colour PuCT – YCbCr colour space at $t = 1$ s PCA image retrieved by PuCT emissivity time series image.

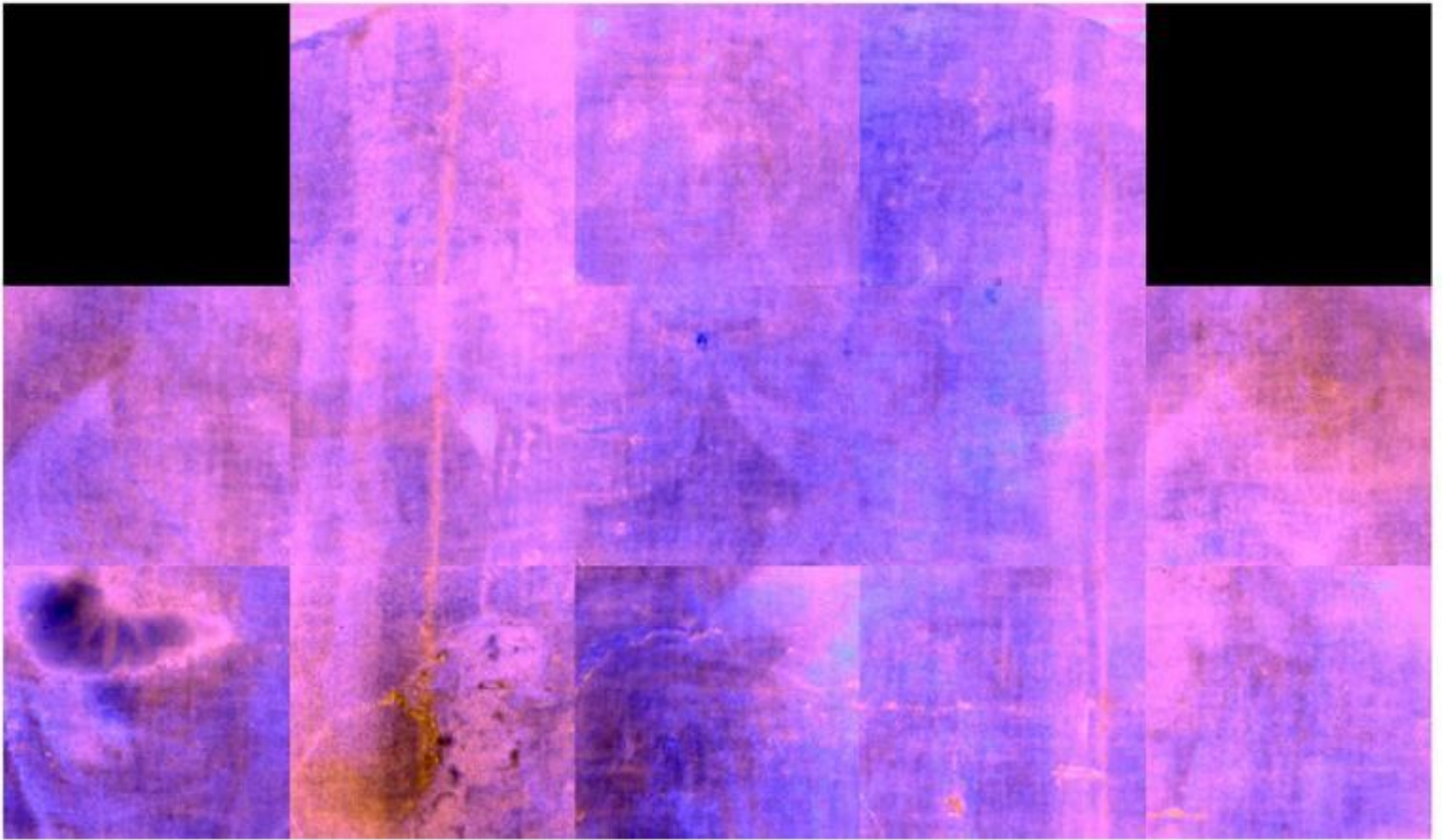


Figure 17

False-colour PuCT – YCbCr colour space at $t = 3$ s PCA image retrieved by PuCT emissivity time series image.



Figure 18

False-colour PuCT – YCbCr colour space at $t = 4$ s PCA image retrieved by PuCT emissivity time series image.